UNIVERSITY OF CALIFORNIA, SAN DIEGO

The Eocene Oligocene Transition: productivity bloom or short-circuit in fishes?

A thesis submitted in partial satisfaction of the
requirements for the Degree Master of Science

in

Earth Sciences

by

Michelle Elizabeth Zill

Committee in charge:

Professor Richard D. Norris, Chair
Professor Peter J. S. Franks
Professor Philip A. Hastings

2016

The Thesis of Michelle Elizabeth Zill is approved, and it is acceptable in quality and form for publication on microfilm and electronically:

_____

_____

_____

Chair

University of California, San Diego

2016

DEDICATION

To my parents, thank you for your endless support.

TABLE OF CONTENTS

LIST OF FIGURES

LIST OF TABLES

ACKNOWLEDGEMENTS

"We're off on the greatest adventure of our lives!" was often exclaimed by Richard Norris whether we were beginning a beach walk, a field trip, or he was simply replying to an email. Well, my time here at Scripps has certainly been a great adventure in my life. I would like to thank Richard Norris for being an excellent advisor. In his paleobiology class, I initially found my passion for paleoceanography. With his supportive guidance and endless enthusiasm, I was able to explore interesting research questions, and discover the type of work I would like to continue with in my career.

I would also like to thank Elizabeth Sibert for all her assistance in my project. Without her pioneering methods, generosity, and patience, my research project would not have gone so smoothly. Her work ethic and passion have long been an inspiration to me, and I am lucky to have been mentored by her.

I would like to thank Peter Franks and Philip Hastings for teaching me about many biological processes that my undergraduate education in the Earth Sciences did not cover. I would like to thank the BS/MS administrators, specifically Jane Teranes and Josh Reeves, for their support throughout my undergraduate and graduate education at Scripps.

I would like to thank everyone in the Norris lab for their comments, and encouragement during my research process. I would like to thank Katie Crammer, Rishi Sugla, Alex Hangsterfer, Kim McComas, and Ted, the assistant lab manager. I would like to thank my family for their encouragement, and Christian Tan for supporting me even when an ocean separates us.

This thesis is currently being prepared for submission for publication of the material. Zill, Michelle E.; Sibert, Elizabeth C.; Norris, Richard D. The thesis author was the primary investigator and author of this material.

ABSTRACT OF THE THESIS

The Eocene Oligocene Transition: productivity bloom or short-circuit in fishes?

by

Michelle Elizabeth Zill

Masters of Science in Earth Science

University of California, San Diego, 2016

Professor Richard D. Norris, Chair

The Eocene-Oligocene Transition (EOT) from 35-33 Ma, centered at 33.9 million years ago (Ma), marks the transition from a Greenhouse to an Icehouse earth. It is associated with the appearance of bulk-feeding whales, and the widespread increase in opal sedimentation in the earliest Oligocene, and has been interpreted to record the initiation of a highly productive Southern Ocean ecosystem. We measured accumulation rates of pelagic fish teeth and shark denticles (ichthyoliths) in a global array of ocean

cores that span the EOT to test the impact of this transition on mid-level pelagic consumers, which could serve as trophic links between the opal-producing diatoms and larger, predatory whales. We find that there is no increase in fish productivity across the Eocene Oligocene Transition in any of our records; indeed, few records show any changes in fish production associated directly with the E/O boundary or the Oi-1 glaciation event at 34 Ma. Moreover, we find that export productivity was lower in our Southern Ocean sites compared to lower latitude sites in both the Atlantic and tropical Pacific for the duration of the records. Ecosystem models predict that diatom-based food webs should support abundant top predators. However, with reduced fish productivity, we speculate that diatoms instead formed the base of a food web which short-circuited fishes, perhaps feeding krill and other seasonally blooming zooplankton that in turn directly supported seasonally present top predators such as large whales.

CHAPTER 1

INTRODUCTION

The Eocene-Oligocene Transition

Fisher and Arthur (1977) and later, Lipps (1986), presented models in which high biological diversity "polytaxic" periods in Earth history, such as the warm Eocene 'greenhouse" gave way to lower diversity, but higher productivity pelagic ecosystems (so called "Oligotaxic" periods) in conjunction with increased glaciation in the Oligocene. Hallock (1986) elaborated on this suggestion that taxonomic diversity in planktonic foraminifera is inversely related to nutrient supply, arguing that plankton do not need to be as specialized in high nutrient waters as they do in oligotrophic waters to successfully compete for nutrients. There is a clear shift in the foraminiferal community from high diversity assemblages in the early Eocene to low species-level diversity during the EOT (Diester-Haass et al., 1996) that generally agrees with Hallock's (1986) model. Indeed, the Eocene-Oligocene boundary (~33.7 Ma) is commonly associated with major diatom sedimentation, along with the appearance of dinoflagellate and nannofossil assemblages indicative of productive coastal Antarctic seas and polar oceans (Villa et al., 2008 Salamy et al., 1999, Plancq et al., 2014).

The establishment of the Southern Ocean ecosystem is associated with the tectonic isolation of Antarctica and subsequent oceanic circulation changes. Tectonic reconstructions of Livermore et al. (2007) show that the Drake Passage substantially opened to deep-sea circulation between 30-34 Ma permitting Pacific waters to invade the South Atlantic. The subsequent influx of nutrients from both the Antarctic continent and deep Pacific waters increased silica availability, and led to a substantial increase in

diatom production in the Southern Ocean. In turn, diatom production initiated a highly productive polar ecosystem, with short, efficient food chains that could support abundant mid and top level consumers—whales, seabirds, seals and fishes (Berger 2007).

Events in the Southern Ocean are connected to global scale changes in Earth's climate. At 34 Ma, a series of $\delta^{18}O$ increases abruptly signal both a drop in temperature and the formation of Antarctica's permanent ice sheet (Zachos et al., 2008). As Antarctica became more isolated, the temperature gradient between the polar and subtropical regions increased (Wei et al., 1991; Mackensen et al., 1992; Zachos et al., 1994). At low latitudes, some regions suggest a decrease in tropical production through the EOT, while other sites see no change in assemblages (Schmidt et al, 2003). At site ODP 1218 in the equatorial Pacific, there is a decrease in silica across the EOT (Salamy et al., 1999), and at ODP site 511 in the South Atlantic, we find a brief increase in opal sedimentation at the EOT that quickly returns to mid-Eocene levels (Plancq et. al, 2014). The radiation of many marine mammals such as bulk-feeding whales suggest that this new, high productivity system in the Oligocene reverberated to the top of the food web. Yet, the response of the trophic link between the two groups, marine mammals and plankton, is relatively unknown.

Introduction to Ichthyoliths

Biological production in the open ocean is commonly estimated with some combination of biological and geochemical proxies. Most biological productivity proxies are based on the abundances of microfossil groups such as diatoms, calcareous nannofossils, and foraminifera, each of which provides an estimate of the export

productivity (that reaching the sediments) of the specific groups of unicellular protists. Common geochemical proxies for biological export production are biogenic barium, % carbonate, % opal, and % total organic carbon. The % opal and % carbonate largely record production by protists, whereas biogenic barium and TOC record export production for the ecosystem as a whole. However, none of the commonly used export production proxies captures the mid-level or upper level parts of pelagic food webs.

Ichthyoliths are an excellent fossil record that bridges this gap by estimating the production of teeth by fishes, which is broadly correlated to fish abundance. We report the abundance of teeth as an "ichthyolith accumulation rate" (IAR) that reflects the number of teeth preserved in a square centimeter of seafloor per million years. By reporting IAR, a measure of fish flux, we can average out long-term changes in sedimentation rates to recover an approximate indication of the production of fishes in the overlying water column at any given point in time. In principle, IAR reflects a number of different aspects of the original fish community including the average longevity of fish in the community, the number of times teeth or denticles are shed in growth of individual fish during its life, and the rate of overall production of fish in the whole community. Our assumption is that IAR is a decent measure of production by the whole fish community given that there are likely to be large variations in longevity and rates of tooth shedding between individual taxa that should average out when considering the fish community as a whole.

Composed of calcium phosphate, these microfossils are highly resistant to dissolution and abundant in deep-sea clays and carbonate. Sibert and Norris (2015) have shown that ~20 cc of pelagic red clay typically contains several hundred to several

thousand teeth in the >38μm size fraction. In pelagic chalk or calcareous ooze, the abundance of teeth is usually less than this, commonly 50-100 teeth in the same size range. Of these, the vast majority, typically > 95%, pass through a 106μm screen reflecting the small size of most ichthyoliths. The abundance of most ichthyoliths means that they can be used to create a high-resolution record, comparable to foraminifera and other microfossils used to investigate export productivity. Furthermore, ichthyoliths are highly resistant to destruction—often representing the last fossils preserved in deep-sea sediments even after all other biogenic carbonates and silica have been dissolved. Hence, teeth and denticles have an unusually extensive fossil record, found in essentially all types of marine sediments. As a consequence of their abundance, preservation and ubiquity in marine sediments, ichthyoliths are a particularly useful paleontological record of past production by mid- and top-level consumers in pelagic food webs.

Here, we directly assess how mid-trophic level fish production changed across the EOT at 5 deep-sea drilling sites around the world, comparing the tropics and subtropical gyres to the Antarctic during this time of intensive global change. We generated high-resolution time series with resolutions of 3.6 to 17.8 samples/million years of pelagic fish tooth abundance in the South Atlantic (Deep Sea Drilling Project (DSDP) Site 522), South Pacific (DSDP Site 596), Equatorial Pacific (Ocean Drilling Program (ODP) Site 1217), and two Southern Ocean sites, Maud Rise, S. Atlantic (DSDP Site 689) and Kerguelen Plateau, Indian Ocean (DSDP Site 748) as shown by Figure 1.

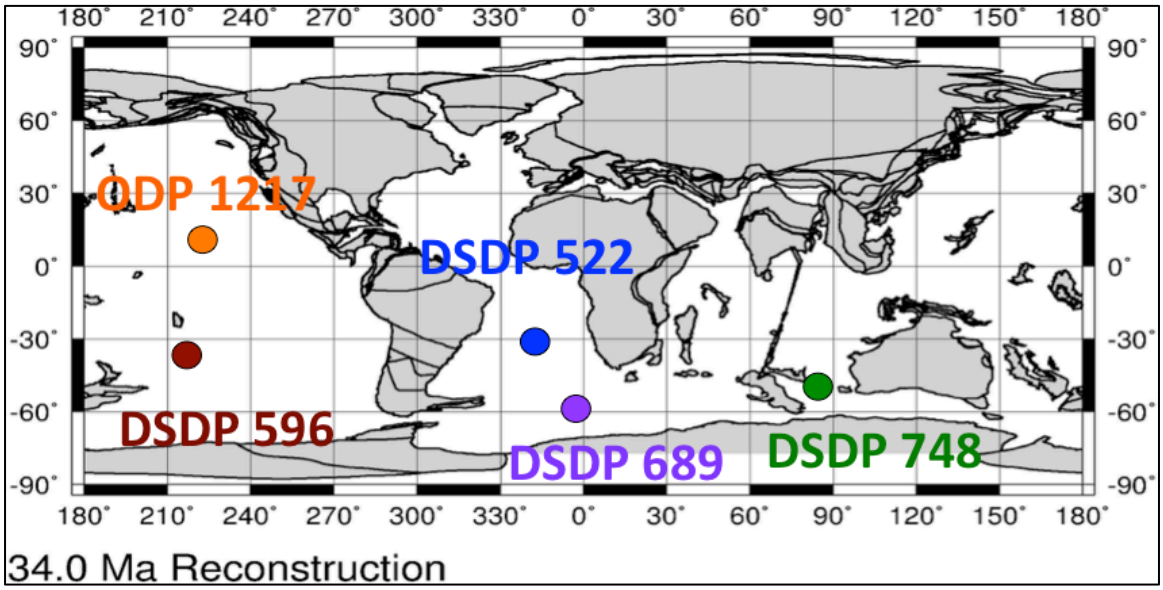

Figure 1: 34.0 Ma plate reconstruction showing paleolocations of study sites DSDP 522, DSDP 596, DSDP 689, DSDP 748, and ODP 1217. Paleomap courtesy of ODSN.

METHODS

All samples were obtained from the International Ocean Discovery Program (IODP). DSDP Site 596 is red clay, DSDP Site 522 is a combination of red clay and carbonate, while DSDP Sites 689, 748, and ODP 1217 are primarily carbonate ooze. Samples were dried to a constant mass (usually ~30 g) in a 50°C oven, weighed, and then the carbonates were removed by dissolution in 7% acetic acid. Samples were checked repeatedly to determine when the carbonate had been completely dissolved (typically 3-4 hours) and then washed over a 38µm sieve, to remove the acid, and concentrate the ichthyoliths. Hence, ichthyoliths were not exposed to low pH for extensive periods of time during processing. Ichthyoliths were then separated into three size fractions, 106µm, 63µm, and 38µm. In the larger two size fractions the ichthyoliths were manually picked and counted, whereas the smallest size fraction (38-63µm) was only counted.

To then convert these raw ichthyolith counts (teeth) into ichthyolith accumulation rates (IAR, ichthyoliths/cm^2-Myr), ichthyolith counts were divided by the original dry sample weight (grams) and multiplied by sedimentation rates (cm/myr) and sediment dry bulk density (g/cm^3) to correct for potential observed changes in ichthyolith abundance due only to sedimentation rate shifts. IAR provides an approximation for the relative abundance of fishes in the overlying water column, and is based on the assumption that average tooth production by different species does not change considerably or systematically over geologic time. The records presented here span a relatively short period in geologic history, further reducing the likelihood that our observed signals are due to a systematic change in average tooth production.

Sedimentation rate for each site is dependent on highly-resolved age constraints. The DSDP 522 time scale is determined based on a paleomagnetic age model (Zachos et al., 1996), as was ODP 1217 (Lyle et al., 2002). The DSDP 596 time scale was based on a cobalt accumulation model tied to the K/Pg boundary (Zhou and Kyte 1992). Both DSDP 689 and DSDP 748 timescales are based on oxygen isotope stratigraphies derived from benthic foraminifera (Mackenson et al., 1992). All timescales were calibrated using the Geologic Timescale 2012 (Gradstein and Ogg 2012).

RESULTS

At DSDP 522, in the South Atlantic gyre, 92 samples were processed across a 5.2 million year interval, spaced about 178 kyr apart in a time series between 35.7 Ma to 30.6 Ma. The material of the core was carbonate with some red clay, and acid-digestion and sieving recovered almost pure samples of teeth. The IAR (Figure 2) falls from an

average of 4500 teeth/cm^2/myr before 33.2 Ma to 3500 teeth/cm^2/myr in the interval 31-33.2 Ma. We see our highest peak (8000 teeth/cm^2/myr) just after 35 Ma, followed by a steep decline across the next 3 million years. These data strongly suggest that there was a ~30% decline in fish production across the EOT, and into the Oligocene. At nearby South Atlantic core 511, there is a spike of biogenic silica at 33.9 Ma, followed by a sharp decrease for the rest of the early Oligocene (Plancq et al., 2014).

At Site DSDP 596 in the South Pacific gyre, 60 samples were processed covering an 18.8 million year period, which resulted in a spacing of ~310 kyr between samples. The material of this core was red clay that had little other than teeth in the picked residue. The average IAR (Figure 2) is ~275 teeth/cm^2/myr before ~38 Ma—a value that drops gradually to an average of ~175 teeth/cm^2/myr between ~36-28 Ma. The highest peak in IAR (499 teeth/cm^2/myr) occurs at 38 Ma, with a long gradual decline across the EOT, hitting its lowest point around 29 Ma. Around 27 Ma, the record begins to increase. Today, DSDP 596 is in one of the ocean regions with the lowest export production anywhere in the oceans. Hence, it is not surprising that the tooth abundance is much lower than DSDP 522 in the South Atlantic.

In the Antarctic, IAR is typically low at both DSDP 689 (located in the Atlantic sector of the Southern Ocean) and DSDP 748 (from the Kerguelan Rise in the southern Indian Ocean). At DSDP 689, 142 samples were processed over a 14 million year time period (26.7 Ma-41.4Ma), at a spacing of ~98 kyr between samples. At ODP 748, 156 samples were processed over 12.6 million year (30.13-42.8 Ma) for a spacing of ~81 kyr between samples. The material of both sites consisted of carbonate with significant amounts of silica in the samples. The IAR (Figure 2) is about 800 teeth/cm^2/myr between

38.2-41.5 Ma, and decreases by half to 400 teeth/cm^2/myr between 26.7-38 Ma. There are peaks in ichthyolith accumulation at 41.5 Ma and again at ~38.3 Ma that reach about 2300 teeth/cm^2/myr. There are also occasional peaks in IAR (to 1100 teeth/cm^2/myr) at 33.7 and 35.3 Ma which are captured in enough samples to be detected in the 5-point moving average. Similarly, at DSDP 748, the long-term average in IAR is about 150 teeth/cm^2/myr. However, there are also a series of high value IAR pulses, starting at 42 Ma, appearing again at 39 Ma, 36.5 Ma and 31 Ma, which last around 1 myr, that reach IAR values of ~350-826 teeth/cm^2/myr. Notably, none of these peaks match closely with IAR highs in the DSDP 689 or DSDP 522 records, despite the common source of all the age models being high resolution benthic d18O records (backed in DSDP 522 by a well resolved magnetostratigraphy). Hence, it appears that the sites are capturing a record of IAR that is largely independent in each location.

At ODP 1217, in the equatorial Pacific, 120 samples were processed across a 13.2 million year interval (29.1 Ma- 42.3 Ma), for a spacing of 110 kyr between samples. The site material was carbonate, with variable numbers of radiolarians present in the core. The IAR (Figure 2) shows significant variation between an average value of ~500 teeth/cm^2/myr between 37.2 and 42 Ma, a peak value of 8900 teeth/cm^2/myr at 35.5 Ma, followed by a decline to between 1400-1700 teeth/cm^2/myr between 31.4-34.6 Ma. Finally IAR rises to an average of ~3000 teeth/cm^2/myr between 29-31 Ma at the end of our record. The trends in IAR partly agree with the barite accumulation rate at nearby Site ODP1218 which generally tracks IAR except for a peak in barite accumulation at 38.7 Ma. Notably, there is an inverse correlation between IAR and opal accumulation rate at ODP 1217: opal accumulation peaks at about 33 Ma just as IAR reaches its low value

for the Oligocene. This negative correlation between IAR and opal accumulation rate is also seen in ODP 748, reinforcing the observation that fish production and opal production are inversely related.

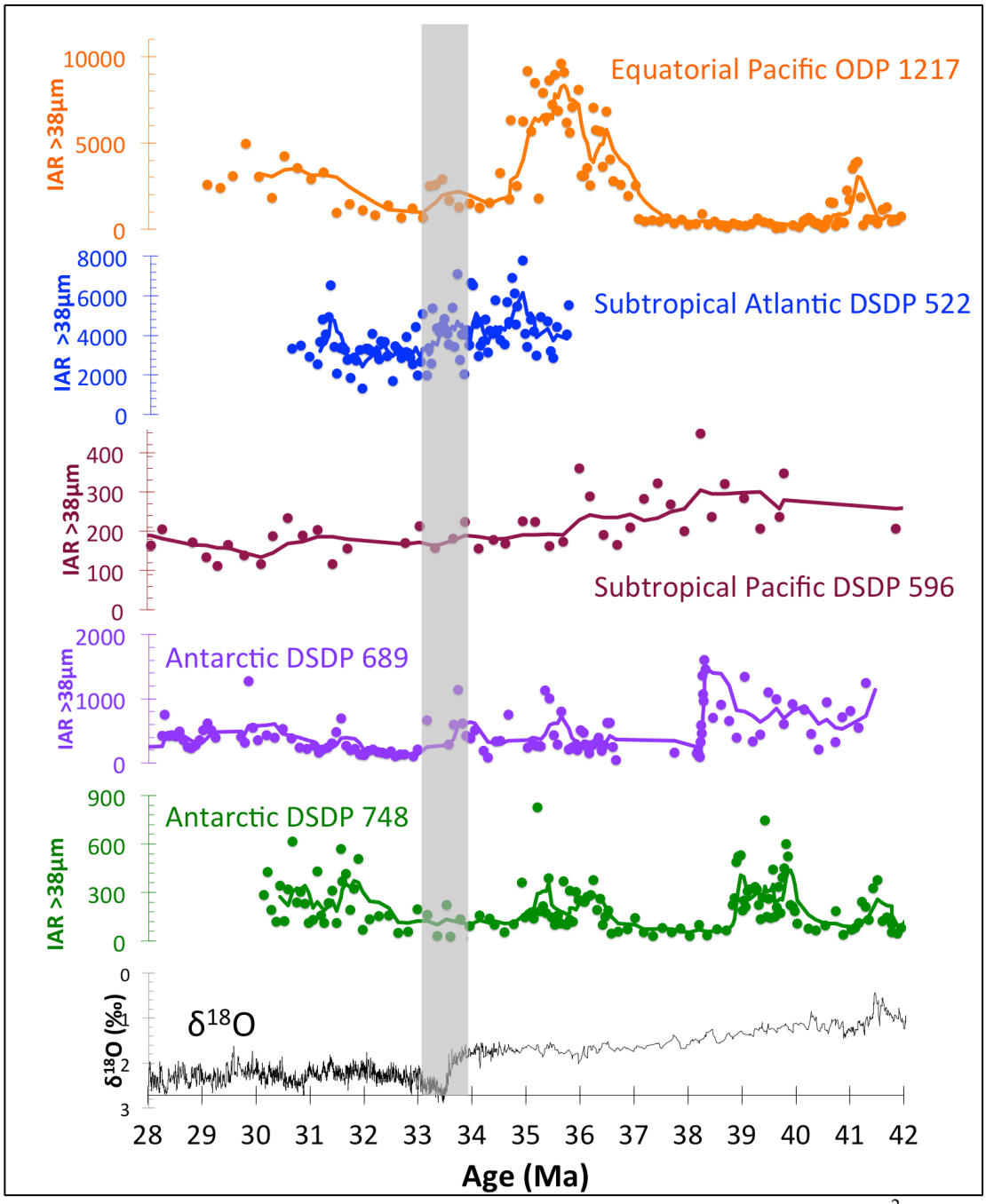

Figure 2: Ichthyolith Accumulation Rate for all sites for ichthyoliths >38µm/cm^2/myr. Oxygen Isotope figure from Zachos et al (2008). All lines are five point moving averages. Gray shaded box is Eocene/Oligocene Transition. All sites were calibrated using the Geologic Time Scale 2012 (GTS 2012).

DISCUSSION

Together, these globally dispersed records of ichthyolith accumulation rate suggest that there is no global change in fish productivity, either increasing or decreasing across the Eocene Oligocene boundary. Hence, while pelagic ecosystems commonly display an increase in biosilica production across the EOT suggesting an increase in primary productivity, this change in production is evidently not translated into a detectable change in fish export production. Further, IAR is generally an order of magnitude lower in the Southern Ocean sites than in the equatorial Pacific or South Atlantic. In the modern Southern Ocean, these sites lie in regions of extremely elevated primary productivity, particularly when compared to the subtropical gyres (Villa et al., 2008). The only site outside the Southern Ocean with comparably low IAR is DSDP 596 in the South Pacific gyre, which is in an ultra-oligotrophic region where one would expect very low productivity.

Taphonomic considerations:

While it is possible that the trends observed in our IAR records are only an artifact of changes in tooth preservation, this is unlikely for several reasons. First, teeth are highly dissolution-resistant. Indeed, the majority of teeth in these samples are almost perfectly preserved, with very few tooth fragments among the samples and generally clear or honey-colored teeth similar to those of living fishes. The only change deviation from excellent preservation was slight blackening of the edges in some teeth from ODP 1217. Second, ichthyoliths are the last fossil group to dissolve, and are found in all oceanic sediments. There is no evidence of rounding or partial dissolution of teeth in any

of the samples, which reflects a lack of transportation after deposition. At hiatuses (define here - I assume intervals missing from cores), there are no significant increases or decreases in IAR, demonstrating that hiatuses have no effect on IAR trends. As each site has tens to hundreds of teeth per sample, it is unlikely that the trends in IAR are simply the result of sampling bias.

Another benefit of this proxy is that it represents a trophic level higher than most productivity proxies. Accumulation rates of common microfossil groups, such as calcareous nannofossils (coccolithophores), dinoflagellates, diatoms, foraminifera and radiolarians, are all representative of unicellular producers or primary consumers, and hence would be expected to largely reflect energy flow at the base of the food web. The same is true for opal or calcium carbonate accumulation rates since these are mainly based on skeletal production by primary producers (like diatoms and coccolithophorids) or low-trophic-level consumers (like foraminifera and radiolarians). Biogenic barium and benthic foraminifera accumulation rates (BFAR) reflect the amount of fixed carbon exported to the seafloor, regardless of biologic source, and are likely more indicative of overall production. In the equatorial Pacific (site 1217), IAR correlates with Ba accumulation (Figure 3), suggesting that IAR may be recording a similar productivity signal as that which is recorded by Ba. This trend of fish IAR correlating with biogenic barium is also observed at several sites across the Cretaceous-Paleogene boundary 66 Ma (Sibert et al 2014), suggesting that the link between IAR and export production is robust, and that IAR is recording a real biological signal.

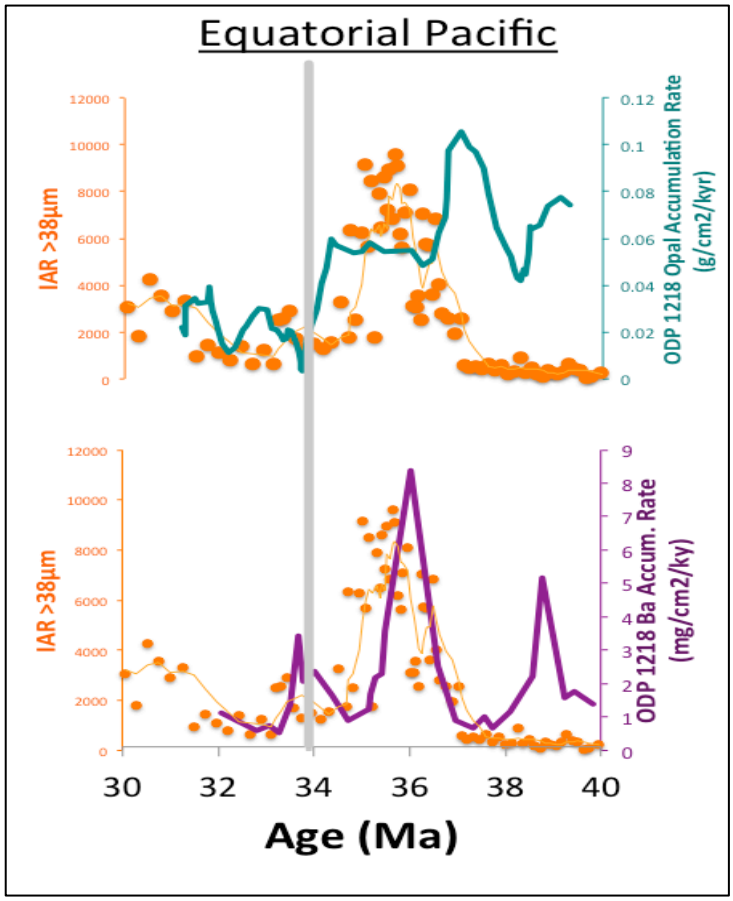

Figure 3: Comparison of IAR ODP site 1217 to ODP site 1218 Opal Accumulation (Moore 2014) and Barium accumulation Rate (Griffith 2010).

Opal production, export production, and fish production

The EOT has long been considered a time of transition from a low-productivity Eocene to high-productivity regime in Antarctic ecosystems. In the Southern Ocean, there is very little opal sedimentation prior to the EOT, however in the Earliest Oligocene, multiple records show a dramatic increase of opal sedimentation rate (Diester-Haas et al., 1996, Salamy et al., 1999). Further, around the EOT, there is an increase in abundance of foraminifera, and a shift from high diversity assemblages in the Eocene to low species-level diversity during the EOT (Diester-Haass 1996). There are also appearances of

dinoflagellate and nannofossil assemblages that indicate that the Antarctic seas and polar oceans were highly productive (Villa et al., 2008, Salamy et al., 1997, Plancq et al., 2014). Yet, Barite and Phosphorus accumulation records in the Southern Ocean indicate increases in export productivity before the EOT, suggesting that the increase in opal sedimentation at the EOT may not be the only relevant productivity signal (Figure 4). Indeed, these records correlate more closely with the IAR records than the opal records do (Faul et al., 2010). In both Southern Ocean IAR records, there are peaks between 38 and 42 Ma that are closely related to the barium and phosphorus records, implying that IAR is responding to total ecosystem productivity, rather than the production of biogenic silica. The peak at 38 Ma is 2 million years after the Mid-Eocene Climatic Optimum (MECO), so it is unlikely to have been linked to the warm climate anomaly.

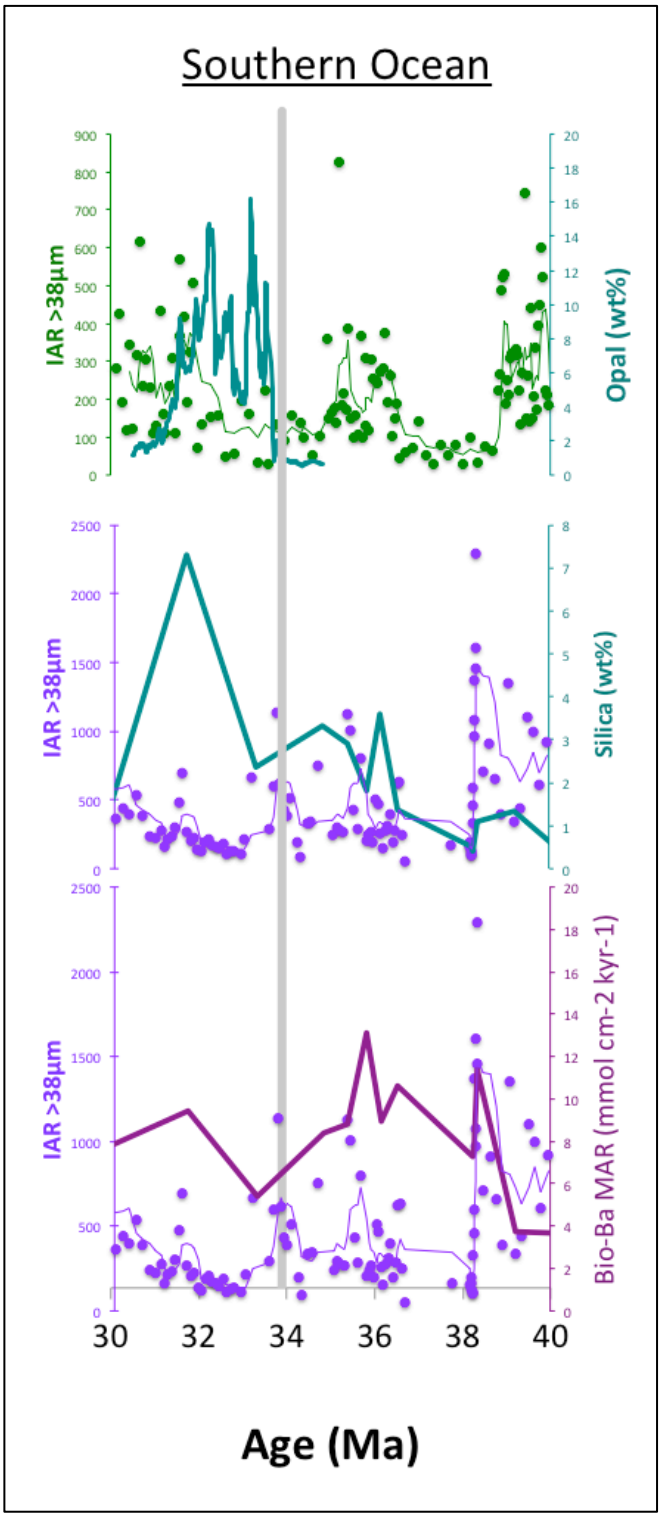

Figure 4: Comparison of IAR of DSDP Sites 689 (purple) against silica weight % and Biological Barium (Faul et al., 2010), and Site DSDP 748 (green) IAR compared to Opal weight % (Salamy et al., 1999).

Both the Equatorial Pacific, South Pacific (Figure 5) and South Atlantic IAR records show a similar pattern, with IAR peaking contemporaneously with barium export (Griffith et al, 2010, Zhou and Kyte1992), but declining during times of increased opal flux, suggesting that the increase in diatom production of the late Eocene and early Oligocene may have short-circuited the food web, moving resources away from higher-level consumers such as fish. Finally, our South Pacific IAR record suggests that the S. Pacific gyre became even less productive for fishes as the Eocene came to a close, although the EOT itself is a non-event in an already highly unproductive ocean.

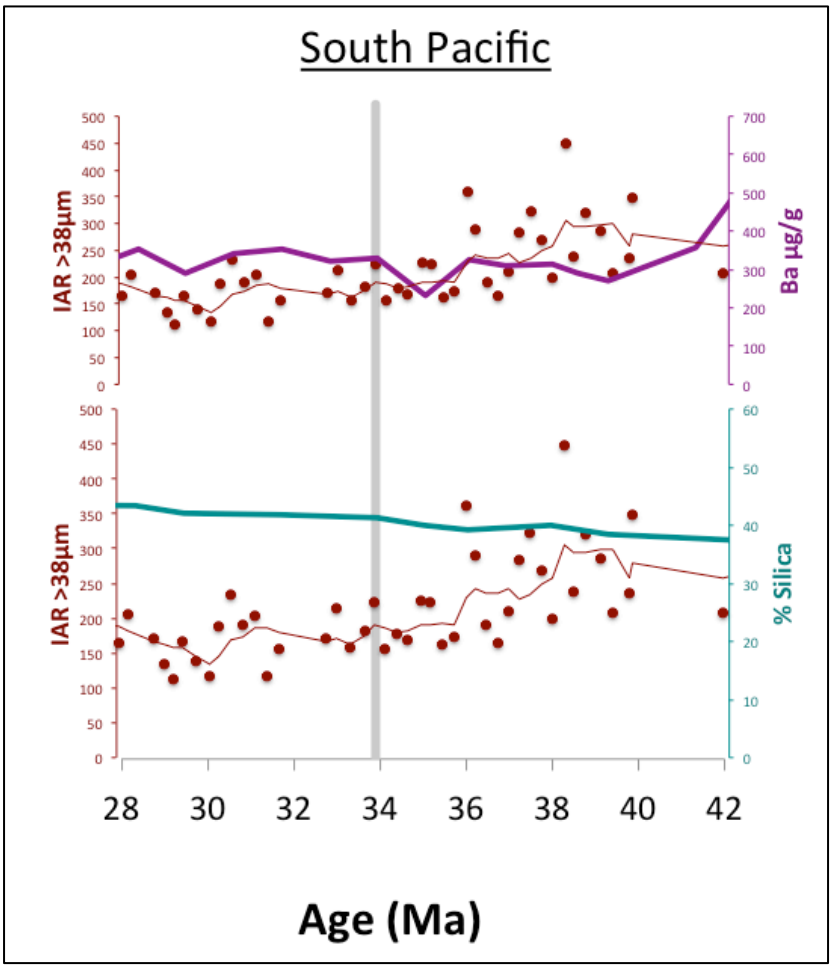

Figure 5: Comparison of IAR DSDP site 596 to percent Silica and Barium (Zhou 1992)

The Paradox of Depressed Southern Ocean Fish Production:

Our records show no increase in fish production, particularly in the Southern Ocean during the EOT, although the increase in diatom production at the EOT has been linked to the diversification of large bulk-feeding whales (Berger 2007). In modern ocean systems, the presence of diatoms indicate a productive, short food chain that more efficiently transfers carbon up trophic levels (Moloney et al., 1991), and is often correlated to high abundances of fish. Yet our records suggest that fishes did not benefit from this ecological shift in phytoplankton. It is possible that fish experience a short-circuit in diatom-based food webs, leading to depressed abundances when diatoms first enter the ecosystem. This short-circuit could either be due to a bottom-up process, such as the zooplankton which they rely on are unable to handle the novel diatom prey, or competitive forces. It is possible that the bulk-feeding whales were more successful in competing with fish for the zooplankton food resource in the new diatom-based food web.

The extremely low abundance of fish in the Southern Ocean throughout the entire interval is another potential paradox, since the modern Southern Ocean is highly productive. However, Antarctica is an extreme environment, with extremely low temperatures and large amounts of sea ice. The EOT represents a several million-year period in which the climate slowly cooled, and the amount of ice gradually increased on Antarctica. Fish would need to adapt to these rapidly changing climatic extremes, and it is possible that as the earth cooled leading up to the EOT, that the Southern Ocean environment became too hostile. Modern Antarctic fish currently deal with the problem of ice crystallization through the adaption of and anti-freeze glycoproteins in the blood stream. Indeed, the lack of fish production observed in the Southern Ocean may be due to

a slow evolution of freeze-resistant fish, and the ecological transition associated with the ecosystem slowly adapting to an ice-dominated habitat. Molecular clock estimates of the timing of origination for Antarctic icefish suggest that the clade developed approximately 42-22 Ma, corresponding roughly to the timing of the EOT, although the error on the age estimate is large (Near et al., 2012). Further, IAR may be depressed in cooler waters, because the lifecycle of fish is slower in cold temperatures. In a system with slow-growing fish and long generation times, there would be fewer teeth reaching the seafloor as individuals die. This could also possibly contribute to the differences in abundances of fish in the lower latitude vs. higher latitude sites.

Indeed, IAR may be somewhat related to global or local temperature. For example, in the Middle Eocene (~41.6–41.3 Ma), there was a short cooling period which was then followed by an abrupt warming event, the Mid Eocene Climatic Optimum (MECO), which was then followed by another sharp cooling event around 39.6 Ma. The Equatorial Pacific shows a small peak in IAR during the MECO, and the Antarctic sites decline considerably at 39 Ma, at the end of the MECO. The South Pacific (site 596) peaks 2 million years later, at 37 Ma, and the South Atlantic (DSDP 522) at 36 Ma. It is possible that fish production begins to decline prior to the EOT because they reached an ecological temperature threshold as the planet cooled, rather than at the EOT.

However, it is likely that overall production, rather than opal production, is a more important factor than local or global temperature in the observed trends in IAR. The microfossil record shows a general decline in productivity across the EOT, but starting much earlier in the Eocene (Wei et al., 1990). For example, after the MECO, there was a switch in nannofossil assemblages, transforming from eutrophic conditions to

oligotrophic conditions, where depressed fish IAR would be expected and is observed (Villa et al., 2013). In the latest Eocene, there is considerable tectonic reorganization in the Southern Ocean, such as the opening of Drake's passage (Livermore et al., 2007). There is evidence for increased upwelling and enhanced nutrient supply during the EOT (Egan 2013), with an increase of iron-rich dust provided from the exposed Antarctic continent. This shift could enhance primary productivity, particularly opal production (Roberts et al., 2011). As IAR in these records is inversely related to opal production, it is likely that this novel productivity regime of the EOT shifted the flux of carbon away from fish, effectively short-circuiting the trophic links to fish and making fixed carbon available for other large marine animals such as whales.

CONCLUSIONS

While the EOT was a time of dramatic climatic change, there is no corresponding change of fish flux at the event itself. Instead, the records seem to support a much more complicated relationship between fish, primary productivity, and changes in global temperature. An ecosystem shift which facilitated considerable increases in diatom abundance and the diversification of our modern whales did not support an elevated level of fish productivity. Rather, it seems as though fish are short-circuited. Indeed our records consistently reveal that the presence of diatoms is inversely correlated with the abundance of fish, suggesting that the newly developing diatom-based food webs were not favorable to fish during the late Eocene and early Oligocene. While there may be an effect of temperature on observed IAR, perhaps reducing the number of teeth produced by slow-growing individuals in cooler waters, the total IAR throughout the interval

appears to be driven more by changes in absolute export productivity, unrelated to the changes in opal production. The observed changes in IAR occur first in the Southern Ocean and reverberate to the Southern Pacific, then the Southern Atlantic, and Equatorial Pacific, suggesting that the EOT was truly a transition, not a rapid boundary event, with changes in fish productivity representing a complex interaction between global temperature, ocean circulation, and changes in the type and abundance of primary producers.

REFERENCES

Berger, W. H. "Cenozoic cooling, Antarctic nutrient pump, and the evolution of whales." *Deep Sea Research Part II: Topical Studies in Oceanography.* 54.21 (2007): 2399-2421.

DeConto, Robert M., and David Pollard. "Rapid Cenozoic glaciation of Antarctica induced by declining atmospheric CO2." *Nature* 421.6920 (2003): 245-249.

Diester-Haass, Liselotte, and Rainer Zahn. "Eocene-Oligocene transition in the Southern Ocean: History of water mass circulation and biological productivity." *Geology* 24.2 (1996): 163-166.

Egan, Katherine E., Rosalind EM Rickaby, Katharine R. Hendry, and Alex N. Halliday. "Opening the gateways for diatoms primes Earth for Antarctic glaciation." *Earth and Planetary Science Letters* 375 (2013): 34-43.

Faul, K. L., and M. L. Delaney. "A comparison of early Paleogene export productivity and organic carbon burial flux for Maud Rise, Weddell Sea, and Kerguelen Plateau, south Indian Ocean." *Paleoceanography* 25.3 (2010).

Fischer, Alfred G., and Michael A. Fisher "Secular variations in the pelagic realm." *The Society of Economic Paleontologists and Mineralogists*. 25 (1977):19-50

Francis, J. E., S. Marenssi, R. Levy, M. Hambrey, V. C. Thorn, B. Mohr, H. Brinkhuis H., Warnaar, J., Zachos, J., Bohaty, S. and DeConto, R., "From greenhouse to icehouse–the Eocene/Oligocene in Antarctica." *Developments in earth and environmental sciences* 8 (2008): 309-368.

Gradstein, Felix M., Gabi Ogg, and Mark Schmitz. *The Geologic Time Scale 2012 2-Volume Set*. Elsevier, 2012.

Griffith, Elizabeth, Michael Calhoun, Ellen Thomas, Kristen Averyt, Andrea Erhardt, Timothy Bralower, Mitch Lyle, Annette Olivarez-Lyle, and Adina Paytan. "Export productivity and carbonate accumulation in the Pacific Basin at the transition from a greenhouse to icehouse climate (late Eocene to early Oligocene)." *Paleoceanography* 25.3 (2010).

Hallock, Pamela, and E. Charlotte Glenn. "Larger foraminifera: a tool for paleoenvironmental analysis of Cenozoic carbonate depositional facies."*Palaios* (1986): 55-64.

Kennett, James P. "Cenozoic evolution of Antarctic glaciation, the circum‐Antarctic Ocean, and their impact on global paleoceanography." *Journal of geophysical research* 82.27 (1977): 3843-3860.

Lear, Caroline Helen, Y. Rosenthal, Helen Kathrine Coxall, and P. A. Wilson. "Late Eocene to early Miocene ice sheet dynamics and the global carbon cycle." *Paleoceanography* 19.4 (2004).

Lipps, Jere H., and Edward Mitchell. "Trophic model for the adaptive radiations and extinctions of pelagic marine mammals." *Paleobiology* 2.02 (1976): 147-155.

Livermore, Roy, Claus‐Dieter Hillenbrand, Mike Meredith, and Graeme Eagles. "Drake Passage and Cenozoic climate: An open and shut case?."*Geochemistry, Geophysics, Geosystems* 8.1 (2007).

Lyle, Mitchell, Samantha Gibbs, Theodore C. Moore, and David K. Rea. "Late Oligocene initiation of the Antarctic circumpolar current: evidence from the South Pacific." *Geology* 35.8 (2007): 691-694.

Mackensen, Andreas, and W. U. Ehrmann. "Middle Eocene through early Oligocene climate history and paleoceanography in the Southern Ocean: Stable oxygen and carbon isotopes from ODP sites on Maud Rise and Kerguelen Plateau." *Marine Geology* 108.1 (1992): 1-27.

Moloney, Coleen L., John G. Field, and Michael I. Lucas. "The size-based dynamics of plankton food webs. II. Simulations of three contrasting southern Benguela food webs." *Journal of Plankton Research* 13.5 (1991): 1039-1092.

Near, Thomas J., Alex Dornburg, Kristen L. Kuhn, Joseph T. Eastman, Jillian N. Pennington, Tomaso Patarnello, Lorenzo Zane, Daniel A. Fernández, and Christopher D. Jones. "Ancient climate change, antifreeze, and the evolutionary diversification of Antarctic fishes." *Proceedings of the National Academy of*

Sciences 109.9 (2012): 3434-3439.

Plancq, Julien, Emanuela Mattioli, Bernard Pittet, Laurent Simon, and Vincent Grossi. "Productivity and sea-surface temperature changes recorded during the late Eocene–early Oligocene at DSDP Site 511 (South Atlantic)."*Palaeogeography, Palaeoclimatology, Palaeoecology* 407 (2014): 34-44.

Robert, Christian, and James P. Kennett. "Antarctic continental weathering changes during Eocene-Oligocene cryosphere expansion: Clay mineral and oxygen isotope evidence." *Geology* 25.7 (1997): 587-590.

Roberts, Andrew P., Fabio Florindo, Giuliana Villa, Liao Chang, Luigi Jovane, Steven M. Bohaty, Juan C. Larrasoaña, David Heslop, and John D. Fitz Gerald. "Magnetotactic bacterial abundance in pelagic marine environments is limited by organic carbon flux and availability of dissolved iron." *Earth and Planetary Science Letters* 310.3 (2011): 441-452.

Salamy, Karen A., and James C. Zachos. "Latest Eocene–Early Oligocene climate change and Southern Ocean fertility: inferences from sediment accumulation and stable isotope data." *Palaeogeography, Palaeoclimatology, Palaeoecology* 145.1 (1999): 61-77.

Schmidt, Daniela N., Hans R. Thierstein, and J. Bollmann. "The evolutionary history of size variation of planktic foraminiferal assemblages in the Cenozoic." *Palaeogeography, Palaeoclimatology, Palaeoecology* 212.1 (2004): 159-180.

Sibert, Elizabeth C., and Richard D. Norris. "New Age of Fishes initiated by the Cretaceous− Paleogene mass extinction." *Proceedings of the National Academy of Sciences* 112.28 (2015): 8537-8542.

Villa, Giuliana, Chiara Fioroni, Davide Persico, Andrew P. Roberts, and Fabio Florindo. "Middle Eocene to Late Oligocene Antarctic glaciation/deglaciation and southern ocean productivity." *Paleoceanography* 29.3 (2014): 223-237.

Wei, Wuchang, and Sherwood W. Wise. "Biogeographic gradients of middle Eocene-Oligocene calcareous nannoplankton in the South Atlantic Ocean."*Palaeogeography, Palaeoclimatology, Palaeoecology* 79.1 (1990): 29-61.

Zachos, James C., Gerald R. Dickens, and Richard E. Zeebe. "An early Cenozoic perspective on greenhouse warming and carbon-cycle dynamics."*Nature* 451.7176 (2008): 279-283.

Zachos, James C., Terrence M. Quinn, and Karen A. Salamy. "High‐resolution (104 years) deep‐sea foraminiferal stable isotope records of the Eocene‐Oligocene

climate transition." *Paleoceanography* 11.3 (1996): 251-266.

Zhou, Lei, and Frank T. Kyte. "Sedimentation history of the South Pacific pelagic clay province over the last 85 million years inferred from the geochemistry of Deep Sea Drilling Project Hole 596." *Paleoceanography* 7.4 (1992): 441-465.

APPENDIX 1. DSDP 522 Data

Table 1: Samples and Data from DSDP 522, Age Model time scale is determined based on a paleomagnetic age model (Zachos et al., 1996).

Sample IODP Identifier	Depth (mbsf)	Age (Ma)	Sample Dry Weight (g)	Teeth	Denticles	Total	IAR
522Z 28H 1W 55-58	104.75	30.63	28.77	80	5	85	3327.36
522Z 28H 2W 57-60	106.27	30.79	30.11	86	7	93	3478.38
522Z 28H 3W 54-56	107.74	30.95	30.6	74	5	79	2907.98
522Z 29H 1W 56-59	109.16	31.1	30.03	61	7	68	2550.25
522Z 29H 1W 100-103	109.6	31.15	29.5	90	6	96	3664.71
522Z 29H 1W 142-144	110.02	31.19	29.77	126	1	127	4804.99
522Z 29H 2W 50-53	110.6	31.26	30.85	102	9	111	4051.87
522Z 29H 2W 103-105	111.13	31.31	30.8	134	1	135	4936.59
522Z 29H 2W 140-143	111.5	31.35	29.63	170	2	172	6536.62
522Z 29H 3W 52-54	112.12	31.42	29.92	90	1	91	3425.44
522Z 29H 3W 100-103	112.6	31.47	30.64	55	1	56	2058.61
522Z 29H CC 11 14	113.21	31.53	30.28	88	2	90	3347.05
522Z 30H 1W 55-58	113.55	31.57	31.64	92	4	96	3416.86
522Z 30H 1W 101-103	114.01	31.62	30.68	85	4	89	3267.35
522Z 30H 1W 140-143	114.4	31.66	30.62	74	1	75	2759
522Z 30H 2W 50-53	115	31.72	27.98	44	2	46	1851.55
522Z 30H 2W 106-108	115.56	31.78	29.93	76	1	77	2897.82

Table 1: Samples and Data from DSDP 522, Age Model time scale is determined based on a paleomagnetic age model (Zachos et al., 1996), Continued

Sample IODP Identifier	Depth (mbsf)	Age (Ma)	Sample Dry Weight (g)	Teeth	Denticles	Total	IAR
522Z 30H 2W 140-143	115.9	31.82	29.83	69	1	70	2718.04
522Z 30H 3W 57-59	116.57	31.89	30.59	88	1	89	3276.27
522Z 30H 3W 100-103	117	31.94	30.57	30	6	36	1326.24
522Z 30H CC 13-16	117.63	32	29.26	72	2	74	3310.16
522Z 31H 1W 56-58	117.96	32.04	30.74	88	3	91	3334.4
522Z 31H 1W 100-103	118.4	32.09	29.62	85	0	85	3232.21
522Z 31H 1W 140-142.5	118.8	32.13	30.7	111	0	111	4072.67
522Z 31H 2W 57-59	119.47	32.2	27.37	72	3	75	3085.63
522Z 31H 2W 100-103.5	119.9	32.25	30.28	74	1	75	2789.81
522Z 31H 2W 137-140	120.27	32.29	29.63	97	0	97	3687.51
522Z 31H 3W 51-54	120.91	32.35	30.64	96	4	100	3675.31
522Z 31H 3W 100-103	121.4	32.41	29.93	76	2	78	2935.35
522Z 32H 1W 51-53	122.31	32.5	33.84	49	2	51	1697.38
522Z 32H 1W 100-103	122.8	32.56	30.65	93	1	94	3454.26
522Z 32H 1W 140-143	123.2	32.6	29.45	83	3	86	3288.74
522Z 32H 2W 57-60	123.87	32.67	28.4	67	5	72	2854.82
522Z 32H 2W 100-103	124.3	32.72	28.06	75	3	78	3130.57
522Z 32H 2W 142-145	124.72	32.76	29.8	100	4	104	3930.7
522Z 32H 3W 53-56	125.33	32.83	28.45	72	1	73	2889.33

Table 1: Samples and Data from DSDP 522, Age Model time scale is determined based on a paleomagnetic age model (Zachos et al., 1996), Continued

Sample IODP Identifier	Depth (mbsf)	Age (Ma)	Sample Dry Weight (g)	Teeth	Denticles	Total	IAR
522Z 32H 3W 100-103	125.8	32.88	30.56	68	1	69	2542.68
522Z 32H CC 42068	126.35	32.93	30.89	118	3	121	4411.42
522Z 33H 1W 50-54	126.7	32.97	30.48	51	2	53	1958.5
522Z 33H 1W 100-103	127.2	33.02	30.3	72	0	72	2675.83
522Z 33H 1W 140-144	127.6	33.07	30.59	135	3	138	5081.18
522Z 33H 2W 57-59	128.27	33.14	30.83	44	7	51	1976.26
522Z 33H 2W 100-103	128.7	33.18	30.78	75	7	82	3360.01
522Z 33H 2W 140-143	129.1	33.22	30.79	63	0	63	2580.39
522Z 33H 3W 17-19	129.37	33.25	30.56	126	4	130	5363.83
522Z 34H 1W 53-58	130.23	33.33	28.39	96	2	98	4353.03
522Z 34H 1W 103-107	130.73	33.38	30.25	96	4	100	4169.23
522Z 34H 1W 138-142	131.08	33.41	30.74	108	1	109	4472
522Z 34H 2W 55-58	131.75	33.47	27.06	101	3	104	4847.45
522Z 34H 2W 106-109	132.26	33.52	29.74	96	0	96	4070.37
522Z 34H 2W 141-143.5	132.61	33.55	30.65	80	6	86	3538.13
522Z 34H 3W 53-57	133.23	33.61	28.18	111	10	121	5415.42
522Z 34H 3W 90-93	133.6	33.65	30.26	82	0	82	3417.4
522Z 35H 1W 51-54	134.21	33.71	31.02	156	7	163	7106.59
522Z 35H 1W 102-107	134.72	33.75	30.55	62	0	62	2762.04

Table 1: Samples and Data from DSDP 522, Age Model time scale is determined based on a paleomagnetic age model (Zachos et al., 1996), Continued

Sample IODP Identifier	Depth (mbsf)	Age (Ma)	Sample Dry Weight (g)	Teeth	Denticles	Total	IAR
522Z 35H 1W 144-146	135.14	33.79	29.26	80	7	87	4046.21
522Z 35H 2W 52-55	135.72	33.84	26.61	37	3	40	2045.77
522Z 35H 2W 100-103	136.2	33.88	30.7	96	0	96	4255.79
522Z 36H 1W 50-53	136.75	33.93	29.41	76	0	76	3516.93
522Z 36H 1W 100-103	137.2	33.97	30.18	146	2	148	6672.82
522Z 36H 1W 140-143	137.6	34.01	30.02	141	3	144	6528.33
522Z 36H 2W 50-53	138.2	34.06	31.46	98	8	106	4586.18
522Z 36H 2W 108-111	138.78	34.11	29.06	61	2	63	2950.56
522Z 36H 2W 140-143	139.1	34.14	30.86	76	3	79	3483.47
522Z 36H 3W 40-50	139.6	34.18	22.71	57	5	62	3714.8
522Z 37H 1W 52-56	140.22	34.24	29.38	103	1	104	4817.63
522Z 37H 1W 100-103	140.7	34.28	29.36	67	1	68	3152.01
522Z 37H 1W 140-143	141.1	34.31	30.79	94	2	96	4243.9
522Z 37H 2W 53-57	141.73	34.37	29.74	84	5	89	4072.82
522Z 37H 2W 100-103	142.2	34.41	29.4	122	3	125	5786.25
522Z 37H 2W 141-143	142.61	34.45	29.25	91	0	91	4233.4
522Z 37H 3W 58-60	143.28	34.51	30.27	79	5	84	3776.52
522Z 38H 1W 55-57	144.25	34.59	30.4	67	12	79	3536.98
522Z 38H 1W 100-102	144.7	34.63	29.25	119	3	122	5675.54

Table 1: Samples and Data from DSDP 522, Age Model time scale is determined based on a paleomagnetic age model (Zachos et al., 1996), Continued

Sample IODP Identifier	Depth (mbsf)	Age (Ma)	Sample Dry Weight (g)	Teeth	Denticles	Total	IAR
522Z 37H 2W 141-143	142.61	34.45	29.25	91	0	91	4233.4
522Z 37H 3W 58-60	143.28	34.51	30.27	79	5	84	3776.52
522Z 38H 1W 55-57	144.25	34.59	30.4	67	12	79	3536.98
522Z 38H 1W 100-102	144.7	34.63	29.25	119	3	122	5675.54
522Z 38H 1W 140-143	145.1	34.67	30.78	103	3	106	4686.2
522Z 38H 2W 57-59	145.77	34.73	28.4	143	1	144	6901.56
522Z 38H 2W 107-110	146.27	34.77	30.01	134	1	135	6122.88
522Z 38H 2W 140-143	146.6	34.8	30.52	101	1	102	4548.09
522Z 38H 3W 17-20	146.87	34.82	28.87	106	10	116	5467.67
522A 29H 1W 56-58	148.06	34.93	26.2	143	7	150	7791.91
522A 29H 1W 100-102	148.5	34.97	29.86	91	0	91	4068.91
522A 29H 1W 140-142	148.9	35	30.81	100	1	101	3416.11
522A 29H 2W 52-54	149.52	35.08	27.52	134	0	134	4788.83
522A 29H 2W 101-103	150.01	35.14	30.3	127	3	130	4220.04
522A 29H 2W 144-146	150.4	35.19	30.59	88	5	93	2990.23
522A 29H 3W 53-55	151.03	35.26	25.59	124	4	128	4919.69
522A 30H 1W 54-56	152.04	35.39	28.2	125	10	135	4709.69
522A 30H 1W 103-105	152.53	35.45	30.85	100	0	100	3188.68
522A 30H 1W 140-143	152.9	35.49	29.77	86	0	86	2841.63

Table 1: Samples and Data from DSDP 522, Age Model time scale is determined based on a paleomagnetic age model (Zachos et al., 1996), Continued

Sample IODP Identifier	Depth (mbsf)	Age (Ma)	Sample Dry Weight (g)	Teeth	Denticles	Total	IAR
522A 30H 2W 53-55	153.53	35.57	27.63	120	4	124	4414.89
522A 31H 1W 53-57	155.03	35.75	29.68	113	9	122	4043.8
522A 31H 1W 82-83	155.32	35.79	30.11	169	0	169	5520.7

APPENDIX 2. DSDP 596 Data

Table 2: Samples and Data from DSDP 596, time scale was based on a cobalt accumulation model tied to the K/Pg boundary (Zhou and Kyte 1992).

Sample IODP Identifier	Depth (mbsf)	Age (Ma)	Sample Dry Weight (g)	Teeth	Denticles	Total	IAR
596 2H 5W 4 6	11.55	23.32	8.4	330	75	405	337.33
596 2H 5W 11 13	11.62	23.55	8.3	233	12	245	206.58
596 2H 5W 16 18	11.67	23.75	6.53	143	6	149	159.8
596 2H 5W 21 23	11.72	23.95	7.41	233	12	245	231.31
596 2H 5W 26 28	11.77	24.21	9.36	227	8	235	175.83
596 2H 5W 32 34	11.83	24.52	7.24	277	19	296	286.38
596 2H 5W 37 39	11.88	24.77	7.65	161	10	171	156.4
596 2H 5W 42 44	11.93	25.03	7.15	207	14	221	216.48
596 2H 5W 45 47	11.96	25.18	9.12	249	7	256	196.46
596 2H 5W 57 59	12.08	25.8	6.14	222	28	250	284.96
596 2H 5W 59 61	12.1	25.9	8.88	296	3	299	235.61
596 2H 5W 65 67	12.16	26.21	9.73	220	15	235	169.14
596 2H 5W 81 83	12.32	27.04	5.88	193	12	205	244.18
596 2H 5W 86 88	12.37	27.3	8.98	300	16	316	246.2
596 2H 5W 90 92	12.41	27.5	11.61	239	6	245	147.72
596 2H 5W 95 97	12.46	27.76	12.56	240	14	254	141.55
596 2H 5W 101 103	12.52	28.07	13.14	300	8	308	164.08

Table 2: Samples and Data from DSDP 596, time scale was based on a cobalt accumulation model tied to the K/Pg boundary (Zhou and Kyte 1992), Continued

Sample IODP Identifier	Depth (mbsf)	Age (Ma)	Sample Dry Weight (g)	Teeth	Denticles	Total	IAR
596 2H 5W 105 107	12.56	28.28	7.52	203	17	220	204.74
596 2H 5W 116 118	12.67	28.85	15.48	372	8	380	171.84
596 2H 5W 121 123	12.72	29.1	15.95	297	9	306	134.33
596 2H 5W 125 127	12.76	29.3	15.06	229	13	242	112.48
596 2H 5W 129 131	12.8	29.5	13.09	284	26	310	165.81
596 2H 5W 135 137	12.86	29.8	19.75	372	19	391	138.55
596 2H 5W 141 143	12.92	30.11	17.76	275	20	295	116.28
596 2H 5W 145 147	12.96	30.33	11.37	293	12	305	187.81
596 2H 6W 0 2	13.01	30.61	6.52	213	4	217	233.05
596 2H 6W 5 7	13.06	30.88	6.53	168	9	177	189.78
596 2H 6W 10 12	13.11	31.16	8.48	233	13	246	203.18
596 2H 6W 15 17	13.16	31.43	8.6	136	8	144	117.17
596 2H 6W 20 22	13.21	31.71	7.77	162	11	173	155.82
596 2H 6W 40 42	13.41	32.78	9.09	214	8	222	170.93
596 2H 6W 45 47	13.46	33.04	8.68	255	10	265	213.63
596 2H 6W 50 53	13.515	33.33	12.16	255	19	274	157.71
596 2H 6W 57 59	13.58	33.67	8.11	200	11	211	182.08
596 2H 6W 60 64	13.62	33.88	6.51	200	8	208	223.71
596 2H 6W 66 68	13.67	34.14	9.1	186	16	202	155.38

Table 2: Samples and Data from DSDP 596, time scale was based on a cobalt accumulation model tied to the K/Pg boundary (Zhou and Kyte 1992), Continued

Sample IODP Identifier	Depth (mbsf)	Age (Ma)	Sample Dry Weight (g)	Teeth	Denticles	Total	IAR
596 2H 6W 71 73	13.72	34.41	8.45	209	6	215	178.08
596 2H 6W 75 77	13.76	34.63	8.99	209	8	217	168.93
596 2H 6W 81 83	13.82	34.96	7.52	220	23	243	226.15
596 2H 6W 85 87	13.86	35.18	7.6	227	16	243	223.68
596 2H 6W 90 92	13.91	35.45	7.9	171	13	184	162.94
596 2H 6W 95 97	13.96	35.7	8.55	193	18	211	172.68
596 2H 6W 101 103	14.02	36	5.59	274	14	288	360.5
596 2H 6W 105 107	14.06	36.2	6.9	257	28	285	289.28
596 2H 6W 110 112	14.11	36.45	8.06	201	19	220	191.06
596 2H 6W 115 117	14.16	36.7	8.15	181	11	192	164.96
596 2H 6W 120 122	14.21	36.95	8.48	243	11	254	209.76
596 2H 6W 125 127	14.26	37.2	8.19	319	12	331	283.04
596 2H 6W 130 132	14.31	37.45	6.93	288	31	319	322.28
596 2H 6W 135 137	14.36	37.7	6.39	235	10	245	268.27
596 2H 6W 140 142	14.41	37.95	8.82	229	23	252	200.03
596 2H 6W 146 148	14.47	38.25	5.75	350	19	369	449.01
596 2H 7W 0 2	14.51	38.45	10.04	323	17	340	237.13
596 2H 7W 5 7	14.56	38.7	5.9	254	16	270	320.25
596 2H 7W 12 14	14.63	39.05	9.31	355	24	379	284.83

Table 2: Samples and Data from DSDP 596, time scale was based on a cobalt accumulation model tied to the K/Pg boundary (Zhou and Kyte 1992), Continued

Sample IODP Identifier	Depth (mbsf)	Age (Ma)	Sample Dry Weight (g)	Teeth	Denticles	Total	IAR
596 2H 7W 18 20	14.69	39.35	6.44	183	8	191	207.47
596 2H 7W 25 27	14.76	39.71	8.96	273	30	303	236.78
596 2H 7W 27 28	14.775	39.78	9.65	455	24	479	347.45
596 2H 1W 6 8	15.17	41.86	4.4	120	10	130	206.86
596 2H 1W 11 13	15.22	42.13	5.87	253	4	257	306.57

APPENDIX 3. DSDP 689 Data

Table 3: Samples and Data from DSDP 689, timescale is based on oxygen isotope stratigraphies derived from benthic foraminifera (Mackenson et al., 1992).

Sample IODP Identifier	Depth (mbsf)	Age (Ma)	Sample Dry Weight (g)	Teeth	Denticles	Total	IAR
689 B 10 H 1 W 10 13	81.8	26.77	16.78	17	0	17	579.51
689 B 10 H 1 W 61 65	82.31	26.85	18.48	8	0	8	247.62
689 B 10 H 1 W 108 112	82.78	26.92	14.89	3	11	14	537.73
689 B 10 H 2 W 6 10	83.26	26.99	29.7	11	0	11	211.83
689 B 10 H 2 W 61 65	83.81	27.07	12.62	18	0	18	815.62
689 B 10 H 2 W 108 112	84.28	27.14	18.39	4	0	4	124.43
689 B 10 H 3 W 10 14	84.8	27.22	23.48	12	0	12	292.37
689 B 10 H 3 W 60 63	85.3	27.29	19.26	15	0	15	445.6
689 B 10 H 3 W 106 111	85.76	27.36	20.85	14	0	14	384.03
689 B 10 H 4 W 10 15	86.3	27.44	33.01	26	0	26	450.59
689 B 10 H 4 W 60 63	86.8	27.51	18.53	10	1	11	339.61
689 B 10 H 4 W 108 112	87.28	27.59	21.26	10	0	10	269
689 B 10 H 5 W 10 13	87.8	27.66	24.23	15	0	15	354.14
689 B 10 H 5 W 60 63	88.3	27.74	28.55	11	0	11	220.4
689 B 10 H 5 W 110 113	88.8	27.81	21.05	11	0	11	298.93
689 B 10 H 6 W 10 13	89.3	27.89	23.12	14	0	14	346.43
689 B 10 H 6 W 60 63	89.8	27.96	16.7	1	0	1	34.25

Table 3: Samples and Data from DSDP 689, timescale is based on oxygen isotope stratigraphies derived from benthic foraminifera (Mackenson et al., 1992), Continued

Sample IODP Identifier	Depth (mbsf)	Age (Ma)	Sample Dry Weight (g)	Teeth	Denticles	Total	IAR
689 B 11 H 1 W 39 44	91.69	28.24	16.86	12	0	12	420.11
689 B 11 H 1 W 70 73	92	28.29	18.52	21	0	21	750.44
689 B 11 H 1 W 120 123	92.5	28.36	17.15	11	0	11	424.46
689 B 11 H 2 W 10 15	92.9	28.42	25.86	17	0	17	435.1
689 B 11 H 2 W 60 63	93.4	28.5	19.34	12	0	12	410.73
689 B 11 H 2 W 109 113	93.89	28.57	21.42	16	0	16	494.29
689 B 11 H 3 W 10 13	94.4	28.64	23.88	13	0	13	360.25
689 B 11 H 3 W 60 63	94.9	28.72	26.49	10	0	10	249.87
689 B 11 H 3 W 110 114	95.4	28.79	25.96	9	0	9	229.46
689 B 11 H 4 W 10 13	95.9	28.87	23.95	10	0	10	276.35
689 B 11 H 4 W 60 63	96.4	28.94	24.1	13	0	13	357.08
689 B 11 H 4 W 110 113	96.9	29.01	16.72	13	0	13	514.65
689 B 11 H 5 W 13 17	97.43	29.09	22.36	19	2	21	621.59
689 B 11 H 5 W 60 63	97.9	29.16	28.48	22	0	22	511.24
689 B 11 H 5 W 115 121	98.45	29.24	24.9	15	0	15	398.71
689 B 12 H 1 W 60 63	101.6	29.71	27.87	17	0	17	403.66
689 B 12 H 1 W 107 110	102.07	29.78	28.69	14	0	14	322.98
689 B 12 H 2 W 9 14	102.59	29.85	21.8	42	0	42	1275.23
689 B 12 H 2 W 60 63	103.1	29.93	26.04	27	0	27	554.35

Table 3: Samples and Data from DSDP 689, timescale is based on oxygen isotope stratigraphies derived from benthic foraminifera (Mackenson et al., 1992), Continued

Sample IODP Identifier	Depth (mbsf)	Age (Ma)	Sample Dry Weight (g)	Teeth	Denticles	Total	IAR
689 B 12 H 2 W 107 110	103.57	30.03	28.98	23	2	25	359.46
689 B 12 H 3 W 10 13	104.1	30.19	27.51	28	1	29	439.23
689 B 12 H 3 W 60 63	104.6	30.34	26.04	25	0	25	400.09
689 B 12 H 3 W 109 112	105.09	30.49	20.29	25	1	26	534.02
689 B 12 H 4 W 10 13	105.6	30.64	24.6	22	1	23	389.58
689 B 12 H 4 W 60 63	106.1	30.79	24.35	14	0	14	239.61
689 B 12 H 4 W 107 110	106.57	30.94	20.91	10	1	11	222.54
689 B 12 H 5 W 12 17	107.12	31.07	20.5	12	1	13	273.67
689 B 12 H 5 W 60 63	107.6	31.15	29.67	11	0	11	160.05
689 B 12 H 5 W 107 112	108.07	31.23	24.16	12	0	12	214.41
689 B 12 H 6 W 11 14	108.61	31.32	29.21	16	0	16	236.45
689 B 12 H 6 W 60 63	109.1	31.4	25.48	18	0	18	304.98
689 B 12 H 6 W 107 110	109.57	31.48	19.82	22	0	22	479.16
689 B 12 H 7 W 10 13	110.1	31.56	18.62	28	2	30	695.39
689 B 13 H 1 W 10 13	110.7	31.66	19.5	12	0	12	265.58
689 B 13 H 1 W 60 63	111.2	31.75	19.18	9	0	9	202.55
689 B 13 H 1 W 106 110	111.66	31.82	23.03	12	0	12	224.95
689 B 13 H 2 W 8 12	112.18	31.91	28.46	9	0	9	136.51
689 B 13 H 2 W 60 65	112.7	32	24.46	7	0	7	123.55

Table 3: Samples and Data from DSDP 689, timescale is based on oxygen isotope stratigraphies derived from benthic foraminifera (Mackenson et al., 1992), Continued

Sample IODP Identifier	Depth (mbsf)	Age (Ma)	Sample Dry Weight (g)	Teeth	Denticles	Total	IAR
689 B 14 H 5 W 15 18	126.35	34.22	22.15	6	0	6	195.2
689 B 14 H 5 W 60 63	126.8	34.29	16.05	2	0	2	89.79
689 B 14 H 6 W 7 10	127.77	34.44	23.75	11	0	11	333.73
689 B 14 H 6 W 55 60	128.25	34.52	18.73	8	1	9	346.22
689 B 14 H 7 W 4 17	129.24	34.67	22.91	24	0	24	754.84
689 B 15 H 2 W 7 11	131.47	35.03	23.86	8	0	8	241.6
689 B 15 H 2 W 63 68	132.03	35.12	21.86	9	0	9	296.72
689 B 15 H 2 W 110 115	132.5	35.19	31.53	12	0	12	274.25
689 B 15 H 3 W 10 13	133	35.27	19.05	7	0	7	264.82
689 B 15 H 3 W 59 62	133.49	35.35	26.82	39	3	42	1128.3
689 B 15 H 3 W 110 115	134	35.43	34.49	48	0	48	1003.03
689 B 15 H 4 W 10 13	134.5	35.51	31.78	19	0	19	430.87
689 B 15 H 4 W 60 63	135	35.59	29.92	12	0	12	289.03
689 B 15 H 4 W 102 108	135.42	35.65	27.85	29	0	29	798.32
689 B 15 H 5 W 65 68	136.55	35.8	26.52	7	0	7	208.38
689 B 15 H 5 W 109 112	136.99	35.84	29.31	9	0	9	242.39
689 B 15 H 6 W 10 13	137.5	35.9	29.83	10	0	10	264.68
689 B 15 H 6 W 60 63	138	35.96	23.95	6	0	6	197.75
689 B 15 H 6W 111 114	138.51	36.01	29.54	19	0	19	507.74

Table 3: Samples and Data from DSDP 689, timescale is based on oxygen isotope stratigraphies derived from benthic foraminifera (Mackenson et al., 1992), Continued

Sample IODP Identifier	Depth (mbsf)	Age (Ma)	Sample Dry Weight (g)	Teeth	Denticles	Total	IAR
689 B 15 H 7 W 8 13	138.98	36.06	21.88	13	0	13	469.02
689 B 16 H 1 W 8 11	139.48	36.12	30.81	10	0	10	256.24
689 B 16 H 1 W 57 63	139.97	36.17	36.65	7	0	7	150.78
689 B 16 H 1 W 111 115	140.51	36.23	25.44	9	0	9	279.26
689 B 16 H 2 W 11 14	141.01	36.29	25.74	10	0	10	306.65
689 B 16 H 2 W 60 63	141.5	36.34	27.94	14	0	14	395.61
689 B 16 H 2 W 113 116	142.03	36.4	20.25	5	0	5	194.89
689 B 16 H 3 W 10 13	142.5	36.45	30.94	11	0	11	280.68
689 B 16 H 3 W 59 62	142.99	36.5	20.26	16	0	16	623.56
689 B 16 H 3 W 105 108	143.45	36.55	21.24	16	1	17	631.77
689 B 16 H 4 W 9 12	143.99	36.61	25.55	8	0	8	247.15
689 B 16 H 4 W 60 63	144.5	36.67	25.93	7	0	7	49.99
689 B 16 H 4 W 105 108	144.95	37.75	22.02	12	0	12	166.89
689 B 16 H 5 W 10 13	145.5	38.17	31.15	9	1	10	156.63
689 B 16 H 5 W 60 63	146	38.18	18.08	6	0	6	161.94
689 B 16 H 5 W 105 111	146.45	38.19	19.98	7	1	8	195.41
689 B 16 H 6 W 10 13	147	38.2	22.42	6	0	6	130.58
689 B 16 H 6 W 59 62	147.49	38.21	30.45	7	0	7	112.16
689 B 16 H 6 W 109 112	147.99	38.23	19.49	4	0	4	100.14

Table 3: Samples and Data from DSDP 689, timescale is based on oxygen isotope stratigraphies derived from benthic foraminifera (Mackenson et al., 1992), Continued

Sample IODP Identifier	Depth (mbsf)	Age (Ma)	Sample Dry Weight (g)	Teeth	Denticles	Total	IAR
689 B 16 H 7 W 9 12	148.49	38.24	17.84	12	0	12	328.27
689 B 17 H 1 W 12 15	149.22	38.25	24.66	28	2	30	593.62
689 B 17 H 1 W 60 63	149.7	38.26	24.25	21	2	23	462.77
689 B 17 H 1 W 108 111	150.18	38.27	27.45	74	3	77	1368.96
689 B 17 H 2 W 10 13	150.7	38.29	19.47	38	5	43	1077.93
689 B 17 H 2 W 60 63	151.2	38.3	24.67	44	5	49	969.07
689 B 17 H 2 W 109 112	151.69	38.31	28.82	90	5	95	1608.47
689 B 17 H 3 W 10 13	152.2	38.32	26.79	119	7	126	2294.93
689 B 17 H 3 W 60 64	152.7	38.33	27.56	74	1	75	1457.63
689 B 17 H 3 W 110 113	153.2	38.47	29.6	38	1	39	709.91
689 B 17 H 4 W 10 13	153.7	38.62	20.93	52	4	56	913.93
689 B 17 H 4 W 60 63	154.2	38.77	31.2	59	1	60	656.68
689 B 17 H 4 W 108 112	154.68	38.91	30.56	35	0	35	391.08
689 B 17 H 5 W 10 13	155.2	39.06	22.01	85	2	87	1349.66
689 B 17 H 5 W 60 66	155.7	39.21	29.12	26	3	29	340.16
689 B 17 H 5 W 108 111	156.18	39.35	28.56	37	0	37	442.38
689 B 17 H 6 W 10 13	156.7	39.5	23.53	74	2	76	1102.92
689 B 17 H 6 W 60 65	157.2	39.64	21.87	59	5	64	999.39
689 B 17 H 6 W 108 111	157.68	39.79	28.05	49	1	50	608.69

Table 3: Samples and Data from DSDP 689, timescale is based on oxygen isotope stratigraphies derived from benthic foraminifera (Mackenson et al., 1992), Continued

Sample IODP Identifier	Depth (mbsf)	Age (Ma)	Sample Dry Weight (g)	Teeth	Denticles	Total	IAR
689 B 17 H 7 W 10 13	158.2	39.94	27.4	71	3	74	922.43
689 B 18 H 1 W 17 20	158.97	40.16	24.98	57	4	61	834.1
689 B 18 H 1 W 60 63	159.4	40.29	28.47	36	2	38	455.9
689 B 18 H 1 W 107 110	159.87	40.43	27.66	16	1	17	209.9
689 B 18 H 2 W 10 13	160.4	40.58	20.58	56	1	57	945.72
689 B 18 H 2 W 63 67	160.93	40.74	29.07	27	1	28	328.98
689 B 18 H 2 W 108 113	161.38	40.87	22.81	48	0	48	718.66
689 B 18 H 3 W 7 10	161.87	41.01	21.82	49	3	52	814.03
689 B 18 H 3 W 60 63	162.4	41.17	22.47	36	0	36	547.26
689 B 18 H 3 W 107 110	162.87	41.31	23.96	79	3	82	1249.58
689 B 18 H 4 W 10 13	163.4	41.48	27.95	160	6	166	2365.61

APPENDIX 4. DSDP 748 Data

Table 4: Samples and Data from DSDP 748, timescale is based on oxygen isotope stratigraphies derived from benthic foraminifera (Mackenson et al., 1992).

Sample IODP Identifier	Depth (mbsf)	Age (Ma)	Sample Dry Weight (g)	Teeth	Denticles	Total	IAR
748 B 11 H 1 W 11.5 14.5	85.72	30.13	25.45	10	1	11	283.16
748 B 11 H 1 W 61 64	86.21	30.21	27.61	18	0	18	427.03
748 B 11 H 1 W 107 110	86.67	30.28	27.31	8	0	8	191.86
748 B 11 H 2 W 12 15	87.22	30.36	27.2	5	0	5	120.39
748 B 11 H 2 W 60 63	87.7	30.44	28.54	15	0	15	344.2
748 B 11 H 2 W 110 113	88.2	30.51	26.93	5	0	5	121.6
748 B 11 H 3 W 10 13	88.7	30.59	28.85	14	0	14	317.85
748 B 11 H 3 W 60 63	89.2	30.66	26.61	25	0	25	615.26
748 B 11 H 3 W 111 114	89.71	30.74	24.87	9	0	9	237
748 B 11 H 4 W 11 14	90.21	30.82	30.04	14	0	14	305.3
748 B 11 H 4 W 60 63	90.7	30.89	28.35	10	0	10	231.06
748 B 11 H 4 W 109 112	91.19	30.97	29.79	5	0	5	109.92
748 B 11 H 5 W 10 13	91.7	31.05	30.32	6	0	6	129.63
748 B 11 H 5 W 60 63	92.2	31.12	25.77	14	3	17	432.03
748 B 11 H 5 W 110 113	92.7	31.2	28.7	7	0	7	159.74
748 B 11 H 6 W 10 13	93.05	31.25	29.31	5	0	5	111.74
748 B 11 H 6 W 60 63	93.55	31.33	30.68	11	0	11	234.85

Table 4: Samples and Data from DSDP 748, timescale is based on oxygen isotope stratigraphies derived from benthic foraminifera (Mackenson et al., 1992) Continued

Sample IODP Identifier	Depth (mbsf)	Age (Ma)	Sample Dry Weight (g)	Teeth	Denticles	Total	IAR
748 B 11 H 6 W 110 103	94.05	31.4	23.25	10	1	11	309.89
748 B 11 H 7 W 10 13	94.55	31.48	29.31	5	0	5	111.74
748 B 11 H 7 W 60 63	95.05	31.56	28.71	24	1	25	570.4
748 B 12 H 1 W 12 15	95.22	31.58	28.43	16	0	16	368.58
748 B 12 H 1 W 62 65	95.72	31.66	29.83	16	3	19	417.18
748 B 12 H 1 W 110 113	96.2	31.73	30.52	9	0	9	193.18
748 B 12 H 2 W 10 13	96.7	31.81	28.38	14	0	14	323.11
748 B 12 H 2 W 60 63	97.2	31.89	25.76	20	0	20	508.58
748 B 12 H 2 W 112 115	97.72	31.96	27.22	5	0	5	70.75
748 B 12 H 3 W 10 13	98.2	32.09	28.72	11	3	14	136.16
748 B 12 H 3 W 60 63	98.7	32.27	30.87	16	1	17	153.81
748 B 12 H 3 W 112 115	99.22	32.45	28.06	16	0	16	159.25
748 B 12 H 4 W 10 13	99.7	32.63	28.75	5	0	5	48.58
748 B 12 H 4 W 60 63	100.2	32.81	29.07	6	0	6	57.64
748 B 12 H 4 W 109 112	100.69	32.98	30.08	19	2	21	195.01
748 B 12 H 5 W 10 13	101.2	33.16	30.9	18	0	18	162.7
748 B 12 H 5 W 60 63	101.7	33.34	26.51	3	0	3	31.6
748 B 12 H 5 W 109 112	102.19	33.52	25.14	19	1	20	222.21
748 B 12 H 6 W 10 13	102.4	33.59	29.16	3	0	3	28.74

Table 4: Samples and Data from DSDP 748, timescale is based on oxygen isotope stratigraphies derived from benthic foraminifera (Mackenson et al., 1992) Continued

Sample IODP Identifier	Depth (mbsf)	Age (Ma)	Sample Dry Weight (g)	Teeth	Denticles	Total	IAR
748 B 12 H 6 W 60 63	102.9	33.77	26.78	13	0	13	135.58
748 B 12 H 6 W 110 103	103.4	33.95	27.62	9	0	9	91.02
748 B 12 H 7 W 10 13	103.9	34.13	28.25	14	2	16	158.2
748 B 12 H 7 W 60 63	104.4	34.31	26.05	13	0	13	139.37
748 B 13 H 1 W 7 10	104.67	34.41	27.62	10	0	10	101.12
748 B 13 H 1 W 60 63	105.2	34.6	26.59	5	0	5	52.52
748 B 13 H 1 W 107 110	105.67	34.76	30.01	9	0	9	104.16
748 B 13 H 2 W 10 13	106.2	34.92	25.18	10	0	10	359.82
748 B 13 H 2 W 60 63	106.7	34.97	24.47	4	0	4	148.09
748 B 13 H 2 W 120 123	107.3	35.04	27.39	5	0	5	165.4
748 B 13 H 3 W 9 12	107.69	35.08	25.73	5	0	5	176.01
748 B 13 H 3 W 59 62	108.19	35.14	26.03	4	0	4	139.2
748 B 13 H 3 W 120 123	108.8	35.2	27.4	25	0	25	826.43
748 B 13 H 4 W 9 12	109.19	35.25	24.63	5	0	5	183.88
748 B 13 H 4 W 58 61	109.68	35.3	21.03	5	0	5	215.4
748 B 13 H 4 W 109 112	110.19	35.36	25.93	5	0	5	174.65
748 B 13 H 5 W 7 10	110.67	35.41	28.05	12	0	12	387.6
748 B 13 H 5 W 59 62	111.19	35.47	24.47	4	0	4	148.09
748 B 13 H 5 W 109.5 112.5	111.7	35.52	27.5	3	0	3	98.81

Table 4: Samples and Data from DSDP 748, timescale is based on oxygen isotope stratigraphies derived from benthic foraminifera (Mackenson et al., 1992) Continued

Sample IODP Identifier	Depth (mbsf)	Age (Ma)	Sample Dry Weight (g)	Teeth	Denticles	Total	IAR
748 B 13 H 6 W 10 13	112.2	35.58	28.73	5	0	5	157.63
748 B 13 H 6 W 59 62	112.69	35.63	25.16	3	0	3	108.01
748 B 13 H 6 W 110 103	113.2	35.69	27	11	0	11	369.09
748 B 13 H 7 W 10.5 13.5	113.71	35.75	27.5	3	0	3	98.82
748 B 13 H 7 W 59 62	114.19	35.8	27.83	4	0	4	130.2
748 B 14 H 1 W 10 13	114.2	35.8	20.45	7	0	7	310.11
748 B 14 H 1 W 60 63	114.7	35.85	30.1	4	0	4	120.39
748 B 14 H 1 W 119 122	115.29	35.92	26.83	9	0	9	303.85
748 B 14 H 2 W 9 12	115.69	35.96	24.81	7	0	7	255.58
748 B 14 H 2 W 62 65	116.22	36.02	25.44	5	2	7	249.29
748 B 14 H 2 W 110 113	116.7	36.08	29.75	8	0	8	243.62
748 B 14 H 3 W 1 4	117.11	36.12	23.24	7	0	7	272.9
748 B 14 H 3 W 66 69	117.76	36.19	28.81	8	1	9	282.95
748 B 14 H 3 W 107.5 110.5	118.18	36.24	24.15	10	0	10	375.16
748 B 14 H 4 W 14 17	118.74	36.3	28.02	6	0	6	193.99
748 B 14 H 4 W 67 70	119.27	36.36	24.13	7	0	7	262.81
748 B 14 H 4 W 112.5 115.5	119.73	36.41	26.67	3	0	3	101.91
748 B 14 H 5 W 6 9	120.16	36.46	30.36	5	0	5	149.19
748 B 14 H 5 W 60 63	120.7	36.52	24.09	5	0	5	188

Table 4: Samples and Data from DSDP 748, timescale is based on oxygen isotope stratigraphies derived from benthic foraminifera (Mackenson et al., 1992) Continued

Sample IODP Identifier	Depth (mbsf)	Age (Ma)	Sample Dry Weight (g)	Teeth	Denticles	Total	IAR
748 B 14 H 5 W 108 111	121.18	36.57	29.59	3	0	3	44.63
748 B 14 H 6 W 14 17	121.74	36.7	30.19	6	0	6	59.17
748 B 14 H 6 W 64 67	122.24	36.87	20.17	5	0	5	73.82
748 B 14 H 6 W 106.5 109.5	122.67	37.01	25.39	11	1	12	140.73
748 B 14 H 7 W 4 7	123.14	37.17	27.5	5	0	5	54.13
748 B 15 H 1 W 6 9	123.66	37.34	29.12	3	0	3	30.68
748 B 15 H 1 W 58 61	124.18	37.52	30.08	8	0	8	79.18
748 B 15 H 1 W 108 111	124.68	37.68	28.24	5	0	5	52.71
748 B 15 H 2 W 7 10	125.17	37.85	26.65	7	0	7	78.21
748 B 15 H 2 W 57 60	125.67	38.02	29.64	3	0	3	30.14
748 B 15 H 2 W 108 111	126.18	38.19	27.26	9	0	9	98.29
748 B 15 H 3 W 3.5 6.5	126.64	38.34	25.65	3	0	3	34.82
748 B 15 H 3 W 58.5 61.5	127.19	38.53	27.92	7	0	7	74.65
748 B 15 H 3 W 109 112	127.69	38.7	24.38	4	0	4	65.48
748 B 15 H 4 W 5 8	128.15	38.81	29.91	5	0	5	224.95
748 B 15 H 4 W 55.5 58.5	128.66	38.85	25.24	5	0	5	266.62
748 B 15 H 4 W 110 113	129.2	38.89	27.57	10	0	10	488.24
748 B 15 H 5 W 7 10	129.67	38.92	30.78	12	0	12	524.72
748 B 15 H 5 W 55 58	130.15	38.96	27.84	11	0	11	531.83

Table 4: Samples and Data from DSDP 748, timescale is based on oxygen isotope stratigraphies derived from benthic foraminifera (Mackenson et al., 1992) Continued

Sample IODP Identifier	Depth (mbsf)	Age (Ma)	Sample Dry Weight (g)	Teeth	Denticles	Total	IAR
748 B 15 H 5 W 106 109	130.66	39	28.56	4	0	4	188.48
748 B 15 H 6 W 14 17	130.94	39.02	32.18	6	0	6	250.91
748 B 15 H 6 W 69 72	131.49	39.06	25.55	4	0	4	210.71
748 B 15 H 6 W 107 110	131.87	39.09	30.48	7	0	7	309.12
748 B 15 H 7 W 7 10	132.37	39.12	29.33	7	0	7	321.25
748 B 16 H 1 W 67 70	133.77	39.23	28.26	6	1	7	333.36
748 B 16 H 1 W 110 113	134.2	39.26	29.64	7	0	7	317.79
748 B 16 H 2 W 10 13	134.7	39.3	30.03	5	0	5	224.11
748 B 16 H 2 W 60 63	135.2	39.33	30.18	3	0	3	133.77
748 B 16 H 2 W 108 111	135.68	39.37	25.03	5	0	5	268.89
748 B 16 H 3 W 9 12	136.19	39.41	25.28	13	1	14	745.33
748 B 16 H 3 W 70 73	136.8	39.45	26.88	3	0	3	150.2
748 B 16 H 3 W 109 112	137.19	39.48	30.97	6	0	6	260.74
748 B 16 H 4 W 7 10	137.67	39.52	28.33	3	0	3	142.53
748 B 16 H 4 W 67 70	138.27	39.56	21.29	6	1	7	442.5
748 B 16 H 4 W 107 110	138.67	39.59	27.12	3	0	3	148.86
748 B 16 H 5 W 10 13	139.2	39.63	25.78	4	0	4	208.8
748 B 16 H 5 W 61 64	139.71	39.67	28.08	6	1	7	335.45
748 B 16 H 5 W 109.5 112.5	140.2	39.71	30.89	4	0	4	174.27

Table 4: Samples and Data from DSDP 748, timescale is based on oxygen isotope stratigraphies derived from benthic foraminifera (Mackenson et al., 1992) Continued

Sample IODP Identifier	Depth (mbsf)	Age (Ma)	Sample Dry Weight (g)	Teeth	Denticles	Total	IAR
748 B 16 H 6 W 0 3	140.6	39.74	23.95	5	2	7	393.35
748 B 16 H 6 W 50 53	141.1	39.77	29.91	8	2	10	449.94
748 B 16 H 7 W 15 18	141.48	39.8	29.2	12	1	13	599.08
748 B 16 H 7 W 60 63	141.93	39.84	28.3	11	0	11	523.19
748 B 17 H 1 W 8 11	142.68	39.89	24.05	4	0	4	223.85
748 B 17 H 1 W 64 67	143.24	39.93	25.61	4	0	4	210.23
748 B 17 H 1 W 107 110	143.67	39.96	25.21	4	0	4	186.36
748 B 17 H 2 W 7 10	144.17	40.01	26.8	10	0	10	108.21
748 B 17 H 2 W 68.5 71.5	144.79	40.22	26.33	7	0	7	77.1
748 B 17 H 2 W 110 113	145.2	40.36	30.2	7	0	7	67.21
748 B 17 H 3 W 8 11	145.68	40.53	27.36	7	2	9	95.4
748 B 17 H 3 W 67 70	146.27	40.73	31.45	15	5	20	184.42
748 B 17 H 3 W 107 110	146.67	40.87	27.5	3	0	3	37.1
748 B 17 H 4 W 7 10	147.17	41.02	32.88	3	0	3	68.43
748 B 17 H 4 W 60 63	147.7	41.09	27.68	3	0	3	81.28
748 B 17 H 4 W 109 112	148.19	41.15	27.11	4	0	4	110.67
748 B 17 H 5 W 0 3	148.6	41.21	27.7	9	0	9	243.73
748 B 17 H 5 W 54 57	149.14	41.28	28.49	8	0	8	210.61
748 B 17 H 5 W 100 103	149.6	41.34	27.5	5	0	5	129.69

Table 4: Samples and Data from DSDP 748, timescale is based on oxygen isotope stratigraphies derived from benthic foraminifera (Mackenson et al., 1992) Continued

Sample IODP Identifier	Depth (mbsf)	Age (Ma)	Sample Dry Weight (g)	Teeth	Denticles	Total	IAR
748 B 17 H 6 W 13.5 16.5	150.14	41.42	27.86	15	1	16	325.47
748 B 17 H 6 W 58 61	150.58	41.49	23.98	15	1	16	378.1
748 B 17 H 6 W 110 113	151.1	41.59	27.29	4	2	6	124.6
748 B 17 H 7 W 7 10	151.57	41.67	30.7	7	1	8	147.69
748 B 17 H 7 W 60 63	152.1	41.76	32.45	5	1	6	104.78
748 B 18 H 1 W 1 4	152.11	41.76	30.99	3	0	3	54.85
748 B 18 H 1 W 61.5 64.5	152.72	41.87	25.38	2	0	2	44.65
748 B 18 H 1 W 101 104	153.11	41.94	24.88	3	0	3	82.68
748 B 18 H 2 W 9 12	153.69	42.02	27.29	8	2	10	358.02
748 B 18 H 2 W 55 58	154.15	42.07	30.52	3	2	5	160.02
748 B 18 H 2 W 108.5 111.5	154.69	42.13	29.94	3	0	3	97.89
748 B 18 H 3 W 10 13	155.2	42.18	30.51	4	0	4	128.06
748 B 18 H 3 W 50 53	155.6	42.22	29.78	7	0	7	229.61
748 B 18 H 3 W 108 111	156.18	42.28	27	3	0	3	108.54
748 B 18 H 4 W 7 10	156.67	42.33	26.69	15	1	16	585.74
748 B 18 H 4 W 63 66	157.23	42.39	29.86	4	0	4	130.85
748 B 18 H 4 W 107 110	157.67	42.43	28.95	4	0	4	134.96
748 B 18 H 5 W 13 16	158.23	42.49	29.4	7	0	7	232.61
748 B 18 H 5 W 57 60	158.67	42.53	28.21	14	3	17	588.63

Table 4: Samples and Data from DSDP 748, timescale is based on oxygen isotope stratigraphies derived from benthic foraminifera (Mackenson et al., 1992) Continued

Sample IODP Identifier	Depth (mbsf)	Age (Ma)	Sample Dry Weight (g)	Teeth	Denticles	Total	IAR
748 B 18 H 5 W 106 109	159.16	42.58	23.33	9	0	9	376.86
748 B 18 H 6 W 9 12	159.39	42.61	29.04	3	0	3	100.91
748 B 18 H 6 W 58 61	159.88	42.66	27.05	7	0	7	252.78
748 B 18 H 6 W 106 109	160.36	42.71	25.58	5	2	7	267.31
748 B 18 H 7 W 8 11	160.88	42.76	28.57	8	0	8	273.53
748 B 18 H 7 W 59 62	161.39	42.81	29.59	7	0	7	231.09

APPENDIX 5. ODP 1217 Data

Table 5: Sample and Data of ODP 1217, time scale is determined based on a paleomagnetic age model ODP 1217 (Lyle et al., 2002).

Sample IODP Identifier	Depth (mbsf)	Age (Ma)	Sample Dry Weight (g)	Teeth	Denticles	Total	IAR
1217 A 3 H 4 W 10 13	19.6	29.17	19.88	243	3	246	2587.45
1217 A 3 H 4 W 60 63	20.1	29.41	14.11	161	1	162	2399.54
1217 A 3 H 4 W 110 113	20.6	29.65	15.27	223	3	226	3095.03
1217 A 3 H 5 W 10 13	21.1	29.89	17.36	403	8	411	4950.85
1217 A 3 H 5 W 60 63	21.6	30.13	18.86	263	12	275	3049.02
1217 A 3 H 5 W 110 113	22.1	30.37	12.39	106	2	108	1822.7
1217 A 3 H 6 W 10 13	22.6	30.61	17.02	334	12	346	4248.91
1217 A 3 H 6 W 60 63	23.1	30.85	18.54	301	14	315	3551.72
1217 B 2 H 3 W 60 63	23.62	31.1	13.61	181	8	189	2903.09
1217 B 2 H 3 W 110 113	24.12	31.34	11.42	178	3	181	3312.67
1217 B 2 H 4 W 10 13	24.62	31.58	12.2	54	2	56	959.42
1217 B 2 H 4 W 60 63	25.12	31.82	10.52	74	0	74	1470.22
1217 B 2 H 4 W 110 113	25.62	32.06	9.44	49	1	50	1106.87
1217 B 2 H 5 W 10 13	26.12	32.3	10.95	41	1	42	801.93
1217 B 2 H 5 W 60 63	26.62	32.54	12.27	79	2	81	1380.14
1217 B 2 H 5 W 110 113	27.12	32.78	14.18	41	4	45	663.46
1217 A 4 H 2 W 130 133	27.56	33	11.42	56	1	57	1225.42

Table 5: Sample and Data of ODP 1217, time scale is determined based on a paleomagnetic age model ODP 1217 (Lyle et al., 2002), Continued

Sample IODP Identifier	Depth (mbsf)	Age (Ma)	Sample Dry Weight (g)	Teeth	Denticles	Total	IAR
1217 A 4 H 3 W 29 32	28.05	33.2	13.5	22	0	22	662.78
1217 A 4 H 4 W 30 33	28.56	33.34	14.54	86	4	90	2517.35
1217 A 4 H 4 W 70 73	28.96	33.45	12.84	77	4	81	2565.14
1217 A 4 H 4 W 120 123	29.46	33.59	8.83	61	7	68	2886.53
1217 A 4 H 5 W 20 23	29.96	33.74	9.88	60	3	63	1694.09
1217 A 4 H 5 W 70 73	30.46	33.96	8.09	37	2	39	1281.32
1217 A 4 H 5 W 120 123	30.96	34.18	7.87	41	3	44	1486.59
1217 A 4 H 6 W 20 23	31.46	34.4	7.79	37	0	37	1261.93
1217 A 4 H 6 W 70 73	31.96	34.62	8.34	46	2	48	1528.84
1217 A 4 H 6 W 120 123	32.46	34.84	8.56	93	3	96	3271.01
1217 A 4 H 7 W 20 23	32.96	35.03	9.69	40	2	42	1749.57
1217 B 3 H 1 W 110 113	33.06	35.06	9.49	139	10	149	6334.72
1217 B 3 H 2 W 10 13	33.56	35.18	9	51	1	52	2499.54
1217 B 3 H 2 W 60 63	34.06	35.3	11.1	95	5	100	6258.52
1217 B 3 H 2 W 110 113	34.56	35.38	11.91	157	0	157	9156
1217 B 3 H 3 W 10 13	35.06	35.45	15.69	123	5	128	5666.47
1217 B 3 H 3 W 60 63	35.56	35.53	12.78	154	2	156	8481.13
1217 B 3 H 3 W 110 113	36.06	35.6	9.41	24	0	24	1771.76
1217 B 3 H 4 W 10 13	36.56	35.68	13.73	129	6	135	7890.02

Table 5: Sample and Data of ODP 1217, time scale is determined based on a paleomagnetic age model ODP 1217 (Lyle et al., 2002), Continued

Sample IODP Identifier	Depth (mbsf)	Age (Ma)	Sample Dry Weight (g)	Teeth	Denticles	Total	IAR
1217 B 3 H 4 W 60 63	37.06	35.72	10.16	68	4	72	6475.18
1217 B 3 H 4 W 110 113	37.56	35.73	10.49	97	2	99	8622.25
1217 B 3 H 5 W 10 13	38.06	35.74	14.56	94	21	115	7216.59
1217 B 3 H 5 W 60 63	38.56	35.75	11.76	115	0	115	8935.78
1217 B 3 H 5 W 110 113	39.06	35.76	10.92	81	1	82	6862.52
1217 B 3 H 6 W 10 13	39.56	35.76	12.67	130	3	133	9594.94
1217 B 3 H 6 W 60 63	40.06	35.77	12.75	125	2	127	9100.37
1217 B 3 H 6 W 107 110	40.53	35.78	12.27	81	2	83	6182.31
1217 B 3 H 7 W 10 13	41.06	35.79	12.21	74	1	75	5614.43
1217 B 3 H 7 W 50 53	41.46	35.8	11.34	87	1	88	7089.74
1217 B 4 H 1 W 10 13	42.52	35.82	12.1	106	1	107	8081.76
1217 B 4 H 1 W 60 63	43.02	35.83	10.23	32	3	35	3126.49
1217 B 4 H 1 W 110 113	43.52	35.84	9.76	32	1	33	3088.81
1217 B 4 H 2 W 10 13	44.02	35.85	12.91	48	2	50	3538.92
1217 B 4 H 2 W 60 63	44.52	35.86	11.13	30	1	31	2544.75
1217 B 4 H 2 W 111 114	45.03	35.87	10.92	82	2	84	7030.34
1217 B 4 H 3 W 10 13	45.52	35.88	12.29	79	4	83	5739.06
1217 B 4 H 3 W 70 73	46.12	36	10	68	7	75	5686.32
1217 B 4 H 3 W 110 113	46.52	36.21	10.25	49	0	49	3623.95

Table 5: Sample and Data of ODP 1217, time scale is determined based on a paleomagnetic age model ODP 1217 (Lyle et al., 2002), Continued

Sample IODP Identifier	Depth (mbsf)	Age (Ma)	Sample Dry Weight (g)	Teeth	Denticles	Total	IAR
1217 B 4 H 4 W 10 13	47.02	36.47	11.44	101	2	103	6827.43
1217 B 4 H 4 W 60 63	47.52	36.72	9.72	53	1	54	4041.18
1217 B 4 H 4 W 110 113	48.02	36.97	9.22	70	0	70	2808.5
1217 B 4 H 5 W 10 13	48.52	37.1	10.79	75	0	75	2570.94
1217 B 4 H 5 W 60 63	49.02	37.22	10.35	52	2	54	1930.45
1217 B 4 H 5 W 110 113	49.52	37.34	10.86	74	1	75	2554.37
1217 B 5 H 1 W 16 21	49.74	37.4	8.62	12	2	14	600.9
1217 B 5 H 1 W 60 63	50.18	37.51	8.89	11	0	11	457.54
1217 B 5 H 1 W 110 113	50.68	37.63	8.93	13	0	13	538.77
1217 B 5 H 2 W 10 13	51.18	37.75	10.92	13	0	13	440.41
1217 B 5 H 2 W 60 63	51.68	37.88	10.25	17	1	18	649.79
1217 B 5 H 2 W 110 113	52.18	38	9.34	9	0	9	356.4
1217 B 5 H 3 W 10 13	52.68	38.12	10.55	16	0	16	561.03
1217 B 5 H 3 W 60 63	53.18	38.24	10.33	6	0	6	223.13
1217 B 5 H 3 W 110 113	53.68	38.36	9.85	7	0	7	299.69
1217 B 5 H 4 W 10 13	54.18	38.47	10.96	21	2	23	885.17
1217 B 5 H 4 W 60 63	54.68	38.58	9.34	6	0	6	276.07
1217 B 5 H 4 W 110 113	55.18	38.69	9.36	10	0	10	463.1
1217 B 5 H 5 W 10 13	55.68	38.79	9	4	0	4	192.72

Table 5: Sample and Data of ODP 1217, time scale is determined based on a paleomagnetic age model ODP 1217 (Lyle et al., 2002), Continued

Sample IODP Identifier	Depth (mbsf)	Age (Ma)	Sample Dry Weight (g)	Teeth	Denticles	Total	IAR
1217 B 5 H 5 W 60 63	56.18	38.89	9.49	2	0	2	91.43
1217 B 5 H 5 W 110 113	56.68	39	9.75	8	0	8	355.8
1217 A 7 H 4 W 110 113	57.12	39.09	7.16	4	0	4	242.43
1217 A 7 H 5 W 10 13	57.62	39.19	9.22	4	0	4	188.25
1217 A 7 H 5 W 60 63	58.12	39.29	8.12	6	0	6	320.5
1217 A 7 H 5 W 110 113	58.62	39.4	6.12	9	0	9	637.5
1217 A 7 H 6 W 10 13	59.12	39.5	8.57	8	0	8	405.03
1217 A 7 H 6 W 60 63	59.62	39.6	8.54	7	0	7	355.57
1217 A 7 H 6 W 110 113	60.12	39.7	7.32	1	0	1	59.23
1217 A 7 H 7 W 11 14	60.63	39.81	8.19	2	0	2	105.86
1217 B 6 H 1 W 60 63	61.44	39.98	7.27	4	0	4	238.75
1217 B 6 H 1 W 110 113	61.94	40.08	8.46	2	0	2	132.68
1217 B 6 H 2 W 10 13	62.44	40.16	9.93	4	1	5	506.14
1217 B 6 H 2 W 60 63	62.94	40.2	8.21	5	0	5	612.21
1217 B 6 H 2 W 110 113	63.44	40.25	9.05	6	0	6	666.65
1217 B 6 H 3 W 10 13	63.94	40.29	9.38	5	0	5	536.11
1217 B 6 H 3 W 60 63	64.44	40.34	8.56	3	0	3	352.16
1217 B 6 H 3 W 110 113	64.94	40.38	9.01	3	0	3	334.66
1217 B 6 H 4 W 10 13	65.44	40.43	10.7	3	0	3	281.91

Table 5: Sample and Data of ODP 1217, time scale is determined based on a paleomagnetic age model ODP 1217 (Lyle et al., 2002), Continued

Sample IODP Identifier	Depth (mbsf)	Age (Ma)	Sample Dry Weight (g)	Teeth	Denticles	Total	IAR
1217 B 6 H 4 W 60 63	65.94	40.47	10.96	1	0	1	91.76
1217 B 6 H 4 W 110 113	66.44	40.51	8.96	2	0	2	224.37
1217 B 6 H 5 W 10 13	66.94	40.56	10.72	6	0	6	562.7
1217 B 6 H 5 W 60 63	67.44	40.6	9.55	15	0	15	1578.86
1217 B 6 H 5 W 110 113	67.94	40.65	9.76	15	0	15	1545.84
1217 B 6 H 6 W 10 13	68.44	40.69	9.52	2	0	2	211.19
1217 B 6 H 6 W 60 63	68.94	40.74	10.21	5	0	5	492.28
1217 B 6 H 7 W 10 13	69.94	40.83	10.94	4	0	4	367.74
1217 C 6 H 1 W 10 13	70.52	40.88	19.25	42	1	43	2246.1
1217 C 6 H 1 W 60 63	71.02	40.92	8.78	15	0	15	1718.33
1217 C 6 H 1 W 110 113	71.52	40.97	8.83	31	0	31	3528.05
1217 C 6 H 2 W 10 13	72.02	41.01	9.55	34	2	36	3787.88
1217 C 6 H 2 W 60 63	72.52	41.06	9.53	37	0	37	3901.84
1217 C 6 H 2 W 110 113	73.02	41.1	8.65	15	1	16	1859.39
1217 C 6 H 3 W 10 13	73.52	41.15	9.84	4	0	4	238.41
1217 C 6 H 3 W 60 63	74.02	41.22	8.54	9	0	9	591.09
1217 C 6 H 3 W 110 113	74.52	41.3	8.97	9	0	9	562.46
1217 C 6 H 4 W 10 13	75.02	41.39	10.07	5	1	6	334.02
1217 C 6 H 4 W 60 63	75.52	41.47	8.83	18	0	18	1142.35

Table 5: Sample and Data of ODP 1217, time scale is determined based on a paleomagnetic age model ODP 1217 (Lyle et al., 2002), Continued

Sample IODP Identifier	Depth (mbsf)	Age (Ma)	Sample Dry Weight (g)	Teeth	Denticles	Total	IAR
1217 C 6 H 4 W 110 113	76.02	41.55	8.31	18	1	19	1281.09
1217 C 6 H 5 W 10 13	76.52	41.63	9.98	8	0	8	449.49
1217 C 6 H 5 W 60 63	77.02	41.71	9.29	9	0	9	542.94
1217 C 6 H 5 W 110 113	77.52	41.79	7.69	10	0	10	728.58
1217 C 6 H 6 W 10 13	78.02	41.87	9.35	8	0	8	479.5
1217 C 6 H 6 W 60 63	78.52	41.95	8.4	10	0	10	667.5
1217 C 6 H 6 W 110 113	79.02	42.03	8.7	12	0	12	773.21
1217 C 6 H 7 W 10 13	79.52	42.11	10.61	10	1	11	581.46